Bending and free vibration analysis of functionally graded beams on elastic foundations with analytical validation

Lazreg Hadji[*1,2] and Fabrice Bernard [3]

[1] *Laboratory of Geomatics and Sustainable Development, University of Tiaret,14000 Tiaret, Algeria*
[2] *Department of Mechanical Engineering, University of Tiaret, BP 78 Zaaroura, 14000 Tiaret, Algeria*
[3] *University of Rennes, INSA Rennes, Laboratory of Civil Engineering and Mechanical Engineering, France*

Abstract. The novelty of this paper is the use of a simple higher order shear and normal deformation theory for bending and free vibration analysis of functionally graded material (FGM) beams on two-parameter elastic foundation. To this aim, a new shear strain shape function is considered. Moreover, the proposed theory considers a novel displacement field which includes undetermined integral terms and contains fewer unknowns with taking into account the effects of both transverse shear and thickness stretching. Different patterns of porosity distributions (including even and uneven distribution patterns, and the logarithmic-uneven pattern) are considered. In addition, the effect of different micromechanical models on the bending and free vibration response of these beams is studied. Various micromechanical models are used to evaluate the mechanical characteristics of the FG beams for which properties vary continuously across the thickness according to a simple power law. Hamilton's principle is used to derive the governing equations of motion. Navier type analytical solutions are obtained for the bending and vibration problems. Numerical results are obtained to investigate the effects of power-law index, length-to-thickness ratio, foundation parameter, the volume fraction of porosity and micromechanical models on the displacements, stresses, and frequencies.

Keywords: functionally graded material; elastic foundation; shear deformation theory; bending; free vibration; stretching effect

1. Introduction

Nowadays, functionally graded (FG) materials are used in many advanced and important engineering structures. The material composition and volume fraction vary according to the simple rule of mixture i.e., power-law through the thickness. Because of this feature, the FGMs have some advantages such as avoiding the material discontinuity and decreasing the delamination failure, diminishing the stress levels and deflections. Combination of these properties attracts practical application of FGMs in many engineering areas such as aircraft, naval/marine, construction and mechanical engineering (Guerroudj *et al*. 2018).

Therefore, understanding bending and free vibration responses of FG beams becomes an important task. Few researchers have developed elasticity solutions for the analysis of FG beams

---

(Ding *et al*. 2007, Ying *et al*. 2008, Hassaine Daouadji *et al*. 2013) which are analytically very difficult. Therefore, researchers have developed various approximate beam theories which are mathematically simpler compared to elasticity solutions. The Euler-Bernoulli beam theory and the first-order beam theory (Timoshenko 1921) are not suitable for the analysis of thick beams due to neglect of shear deformation effect. Therefore, higher-order beam theories have been developed by various researchers. These theories considered the effect of transverse shear deformation and are accurate for the analysis of thick beams. There exist various classes of higher-order beam theories, which account for the effect of transverse shear deformation, such as parabolic beam theories (Reddy 1984), trigonometric beam theories (Touratier 1991, Mantari *et al*. 2012, Sayyad *et al*. 2015), hyperbolic beam theories (Soldatos 1992, Neves *et al*. 2012), exponential beam theories (Karama *et al*. 2003), etc.

In the last decade, several works have been published by researchers on bending, buckling and free vibration analysis of functionally graded beams (Simsek 2010, Sayyad and Ghugal 2017, 2018, Zouatnia *et al*. 2017, Draiche *et al*. 2019, Karami *et al*. 2018a, b, 2019a, b, c, d, Abualnour *et al*. 2019, Alimirzaei *et al*. 2019, Medani *et al*. 2019, Draoui *et al*. 2019, Berghouti *et al*. 2019, Bourada *et al*. 2019, Batou *et al*. 2019, Tlidji *et al*. 2019, Salah *et al*. 2019, Boussoula *et al*. 2020, Adda Bedia *et al*. 2019, Meksi *et al*. 2019, Hellal *et al*. 2019, Hussain *et al*. 2019, Belbachir *et al*. 2019, Mahmoud *et al*. 2019, Sahla *et al*. 2019). Different models have been proposed to estimate the effective properties of FGMs with respect to reinforcement volume fractions (Shen and Wang 2012, Jha *et al*. 2013). Consequently, several micromechanical models have been used to study and analyze the behavior of FGM structures under different loading conditions. We cite as an example the work of Gasik (1998) in which a micromechanical model is proposed to study FGMs with a random distribution of constituents. Karami *et al*. (2019e) studied the influence of homogenization schemes on vibration of functionally graded curved microbeams. Karami *et al*. (2019f) analyze the static analysis of functionally graded anisotropic nanoplates using nonlocal strain gradient theory. Karami *et al*. (2020a) developed the dynamics of two-dimensional functionally graded tapered Timoshenko nanobeam in thermal environment using nonlocal strain gradient theory. Karami *et al*. (2020b) investigated a novel study on functionally graded anisotropic doubly curved nanoshells.

In addition, in FGM fabrication, micro voids or porosities can occur within the materials during the process of sintering. This is because of the large difference in solidification temperatures between material constituents (Zhu *et al*. 2001). Wattanasakulpong *et al*. (2012) also gave the discussion on porosities happening inside FGM samples made by a multistep sequential infiltration technique. Therefore, it is important to take into account the porosity effect when designing FGM structures subjected to dynamic loadings. Recently, Wattanasakulpong and Ungbhakorn (2014) studied linear and nonlinear vibration problems of elastically end restrained FG beams having porosities. In the same way Ait Yahia *et al*. (2015) investigated the wave propagation of an infinite FG plate having porosities by using various simple higher-order shear deformation theories. Hassaine Daouadji *et al*. (2016) studied the bending analysis of an imperfect FGM plates under hygro-thermo-mechanical loading with analytical validation. Akbaş (2017) analyze the thermal effects on the vibration of functionally graded deep beams with porosity. Karami *et al*. (2018b) used a high-order gradient model for wave propagation analysis of porous FG nanoplates. Karami *et al*. (2017) developed the wave propagation in fully clamped porous functionally graded nanoplates. She *et al*. (2019) studied the nonlinear bending behavior of FG porous curved nanotubes. Karami *et al*. (2020c) analyze the free vibration of FG nanoplate with poriferous imperfection in hygrothermal environment.

To study the behavior of functionally graded beams resting on elastic foundation, several mathematical models have been developed. Ait Atmane *et al.* (2017) studied the effect of thickness stretching and porosity on mechanical response of a functionally graded beams resting on elastic foundations. Khelifa *et al.* (2018) studied the buckling response with stretching effect of carbon nanotube-reinforced composite beams resting on elastic foundation. Sayyad and Ghugal (2018) developed an inverse hyperbolic theory for FG beams resting on Winkler-Pasternak elastic foundation. Zaoui *et al.* (2019) used new 2D and quasi-3D shear deformation theories for free vibration of functionally graded plates on elastic foundation. Recently, Addou *et al.* (2019) studied the influences of porosity on dynamic response of FG plates resting on Winkler/Pasternak/Kerr foundation using quasi 3D HSDT. Chaabane *et al.* (2019) developed an analytical study of bending and free vibration responses of functionally graded beams resting on elastic foundation. Boulefrakh *et al.* (2019) studied the effect of parameters of visco-Pasternak foundation on the bending and vibration properties of a thick FG plate. Boukhlif *et al.* (2019) used a simple quasi-3D HSDT for the dynamics analysis of FG thick plate on elastic foundation. Semmah *et al.* (2019) analyze the thermal buckling of SWBNNT on Winkler foundation by non local FSDT. Karami *et al.* (2019g) investigated the wave propagation of functionally graded anisotropic nanoplates resting on Winkler-Pasternak foundation. Shahsavari *et al.* (2018) used a novel quasi-3D hyperbolic theory for free vibration of FG plates with porosities resting on Winkler/Pasternak/Kerr foundation. Mahmoudi *et al.* (2019) used a refined quasi-3D shear deformation theory for thermomechanical behavior of functionally graded sandwich plates on elastic foundations. In addition, in recent years, many researchers have dealt the effect of stretching the thickness on FGM structures (Boutaleb *et al.* 2019, Khiloun *et al.* 2019, Zarga *et al.* 2019, Boulefrakh *et al.* 2019, Boukhlif *et al.* 2019, Mahmoudi *et al.* 2019, Zaoui *et al.* 2019).

The purpose of this study is to establish a simple higher order shear and normal deformation theory to investigate the bending and free vibration of FG beams on elastic foundation. The novelty of this theory is the use of a new shear strain shape function which considers an adequate distribution of the transverse shear strains across the beam thickness and tangential stress-free boundary conditions on the beam boundary surface without introducing a shear correction factor. Undetermined integral terms are employed in the proposed displacement field in which the normal stresses effects are considered in the present shear deformation theory. Different patterns of porosity distributions (including even and uneven distribution patterns, and the logarithmic-uneven pattern) are considered. In addition, the effect of different micromechanical models on the bending and free vibration response of these beams is studied. Various micromechanical models are used to evaluate the mechanical characteristics of the FG beams of which properties vary continuously across the thickness according to a simple power law. The equations of motion of FG plates resting on elastic foundation are obtained from the Hamilton's principle and solved via Navier's procedure. Analytical solutions for static and free vibration are obtained. The effects of various variables, such as span-to-depth ratio, gradient index, foundation parameter, the volume fraction of porosity and micromechanical models on bending and free vibration of FG beam are all discussed.

2. Effective properties of FGMs

Unlike traditional microstructures, in FGMs the material properties are spatially varying, which is not trivial for a micromechanics model (Jaesang and Addis 2014).

A number of micromechanics models have been proposed for the determination of effective

properties of FGMs. In what follows, we present some micromechanical models to calculate the effective properties of the FG beam.

2.1 Voigt model

The Voigt model is relatively simple; this model is frequently used in most FGM analyses that estimate young's modulus E of FGMs as (Mishnaevsky 2007)

$$E(z) = E_c V_c + E_m(1 - V_c) \tag{1}$$

2.2 Reuss mode

Reuss assumed the stress uniformity through the material and obtained the effective properties as (Mishnaevsky 2007, Zimmerman 1994)

$$E(z) = \frac{E_c E_m}{E_c(1 - V_c) + E_m V_c} \tag{2}$$

2.3 Tamura model

The Tamura model uses actually a linear rule of mixtures, introducing one empirical fitting parameter known as "stress-to-strain transfer" (Gasik 1995)

$$q = \frac{\sigma_1 - \sigma_2}{\varepsilon_1 - \varepsilon_2} \tag{3}$$

Estimate for $q = 0$ corresponds to Reuss rule and for $q = 100$ to the Voigt rule, being invariant to the consideration of which phase is matrix and which is particle. The effective Young's modulus is found as

$$E(z) = \frac{(1 - V_c)E_m(q - E_c) + V_c E_c(q - E_m)}{(1 - V_c)(q - E_c) + V_c E_c(q - E_m)} \tag{4}$$

2.4 Description by a representative volume element (LRVE)

The local representative volume element (LRVE) is based on a "mesoscopic" length scale which is much larger than the characteristic length scale of particles (inhomogeneities) but smaller than the characteristic length scale of a macroscopic specimen (Ju and Chen 1994). The LRVE is developed based on the assumption that the microstructure of the heterogeneous material is known. The input for the LRVE for the deterministic micromechanical framework is usually volume average or ensemble average of the descriptors of the microstructures.

Young's modulus is expressed as follows by the LRVE method (Akbarzadeh *et al*. 2015)

$$E(z) = E_m \left(1 + \frac{V_c}{FE - \sqrt[3]{V_c}} \right), \qquad FE = \frac{1}{1 - \frac{E_m}{E_c}} \tag{5}$$

2.5 Mori-Tanaka model

The locally effective material properties can be provided by micromechanical models such as the Mori–Tanaka estimates. This method considers the heterogeneous material as a two-phase composite one consisting of a matrix reinforced by spherical particles, randomly distributed in the plate. According to the Mori-Tanaka homogenization scheme, the Young's modulus is given by

$$E(z) = E_m + (E_c - E_m)\left(\frac{V_c}{1 + (1 - V_c)(E_c/E_m - 1)(1 + v)/(3 - 3v)}\right) \tag{6}$$

Where $V_c = \left(\frac{1}{2} + \frac{z}{h}\right)^p$ is the volume fraction of the ceramic and where p is the power law index. Since the effects of the variation of Poisson's ratio (v) on the response of FGM plates are very small (Kitipornchai 2006), this material parameter is assumed to be constant for convenience.

3. Mathematical modeling

3.1 Functionally graded beams

In this work, a rectangular beam of uniform thickness h, length L and rectangular cross section $b \times h$, made of FGM and supported by an elastic foundation is considered, as shown in Fig. 1.

3.2 Constitutive relations

The effective material characteristics of the beam, such as Young's modulus E and material density ρ which are assumed to change smoothly across the thickness according to a power law distribution (see Fig. 2), can be evaluated using the following rule of mixture

$$P(z) = P_b + (P_t - P_b)\left(\frac{z}{h} + \frac{1}{2}\right)^p - P_{por} \tag{7}$$

where P signifies the effective material property, P_t and P_b represent the property of the top and bottom faces of the beam, respectively, and p is the power-law index that specifies the material distribution profile within the thickness. The Poisson's ratio v, is usually considered to be constant (Delale and Erdogan 1983, Sallai *et al.* 2009).
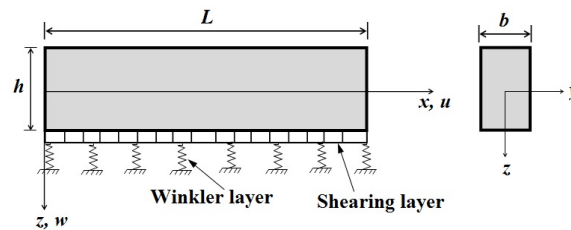

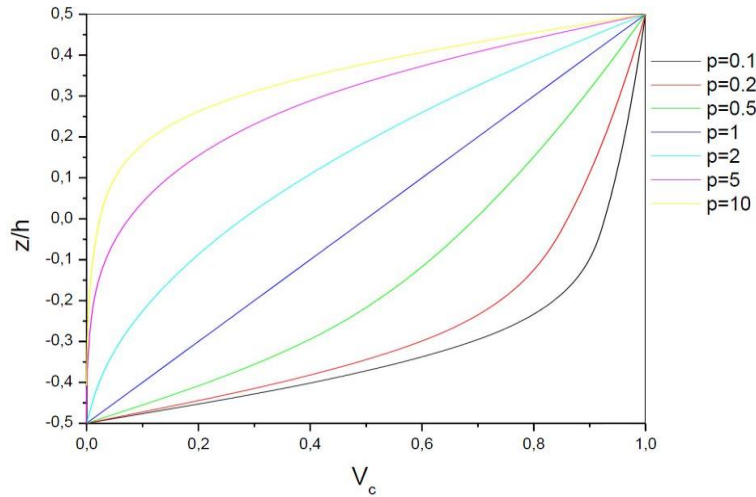Fig. 1 FGM Beam resting on a two parameters elastic foundation

Fig. 2 Functionally graded function $V_c = \left(\frac{z}{h} + \frac{1}{2}\right)^p$ through the thickness of a FGM beam for different values of the index (p)

(a)   (b)

Fig. 3 Porosity models: (a) Evenly distributed porosities; (b) Unevenly distributed porosities

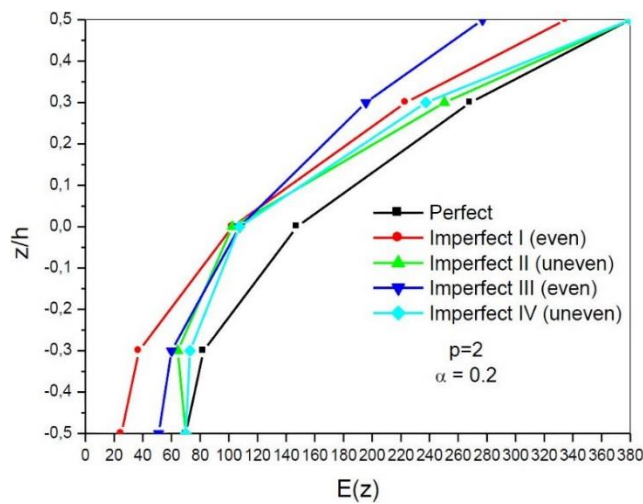
Fig. 4 Variation of Young's modulus $E(z)$ through the thickness of embedded perfect and imperfect FG beams ($p = 2$ and $\alpha = 0.2$)

In this study, four types of porosity are considered, some of them present an evenly distribution (called hereafter Imperfect I and III), whereas the other ones are characterized by an unevenly distribution (Imperfect II and IV hereafter), along the beam thickness direction (Fig. 3).

- Imperfect-I:

$$P_{por} = \frac{\alpha}{2}(P_c + P_m) \tag{8}$$

- Imperfect II:

$$P_{por} = \frac{\alpha}{2}\left(1 - \frac{2|z|}{h}\right)(P_c + P_m) \tag{9}$$

- Imperfect III:

$$P(z) = \left((P_c - P_m)\left(\frac{z}{h} + \frac{1}{2}\right)^p + P_m\right)\left(1 - \frac{\alpha}{2}\right)^3 \tag{10}$$

- Imperfect IV:

$$P(z) = \left((P_c - P_m)\left(\frac{z}{h} + \frac{1}{2}\right)^p + P_m\right)\left(1 - \frac{\alpha}{2}\left(1 - 2\frac{|z|}{h}\right)\right)^3 \tag{11}$$

Imperfect III and IV models are an adaptation of widely used expressions for porous geomaterials, such as cement-based materials (Kendall *et al*. 1983).

Fig. 4 illustrates the variation of Young's modulus $E(z)$ through the thickness of embedded perfect and imperfect FG beams for the various porosity distributions considered in this work and for a constant value of the power law index $(p = 2)$.

3.3 Kinematic and constitutive relations

Based on the formulation proposed by Zaoui *et al*. (2019), the displacements field of the proposed theory is expressed by

$$u(x, z, t) = u_0(x, t) - z\frac{\partial w_0}{\partial x} + k_1 f(z)\int \theta(x, t)\, dx \tag{12a}$$

$$w(x, z, t) = w_0(x, t) + g(z)\varphi_z(x, t) \tag{12b}$$

Where u_0 and w_0 are mid-plane displacements, θ and φ_z are rotations of normals to the mid-plane of the beam. Note that the integrals do not have limits.

In this study, two simple higher order shear and normal deformation theories $f(z)$ are developed as given in Eqs. (13a) and (13b) (Mechab *et al*. 2017). These two new models assure an accurate distribution of shear deformation according to the beam thickness and consider parabolic transverse shear stresses across the thickness as satisfying shear stress free surface conditions without including shear correction factors.

$$f(z) = \frac{3}{2}\pi h \tanh\left(\frac{z}{h}\right) - \frac{3}{2}\pi z \sec h\left(\frac{1}{2}\right)^2 \tag{13a}$$

$$\boldsymbol{f(z)} = \frac{\cosh\left(\frac{\pi}{2}\right)}{\left(\cosh\left(\frac{\pi}{2}\right) - 1\right)} z - \frac{h}{\pi} \frac{\sinh\left(\frac{\pi}{h}z\right)}{\left(\cosh\left(\frac{\pi}{2}\right) - 1\right)} \tag{13b}$$

and

$$g(z) = \frac{df(z)}{dz} \tag{13c}$$

The strains associated with the displacements in Eq. (1) are

$$\varepsilon_x = \varepsilon_x^0 + z\,k_x^b + f(z)\,k_x^s \tag{14a}$$

$$\gamma_{xz} = g(z)\,\gamma_{xz}^0 \tag{14b}$$

$$\varepsilon_z = g^{'}(z)\varepsilon_z^0 \tag{14c}$$

Where

$$\varepsilon_x^0 = \frac{\partial u_0}{\partial x} \tag{15a}$$

$$k_x^b = -\frac{\partial^2 w_0}{\partial x^2} \tag{15b}$$

$$k_x^s = k_1\theta \tag{15c}$$

$$\gamma_{xz}^0 = k_1 \int \theta\,dx + \frac{\partial\varphi_z}{\partial x} \tag{15d}$$

$$\varepsilon_z^0 = \varphi_z \tag{15e}$$

The integrals appearing in the above expressions are solved by using Navier's type solution and can be expressed as (Mantari *et al*. 2016)

$$\int \theta\,dx = A'\frac{\partial\theta}{\partial x} \tag{16}$$

Where the coefficient A' is expressed according to the type of solution used, in this case via Navier procedure. Therefore, A' and k_1 are expressed as follows

$$A' = -\frac{1}{\alpha^2}, \quad k_1 = \alpha^2 \tag{17}$$

Where α is defined in expression (22).

The stress–strain relationships for the FG beams are as follows

$$\sigma_x = Q_{11}(z)\,\varepsilon_x + Q_{13}(z)\,\varepsilon_z \tag{18a}$$

$$\sigma_z = Q_{13}(z)\,\varepsilon_x + Q_{33}(z)\,\varepsilon_z \tag{18b}$$

$$\tau_{xz} = Q_{55}(z)\,\gamma_{xz} \tag{18c}$$

The Q_{ij} expressions in terms of engineering constants are

$$Q_{11}(z) = Q_{33}(z) = E(z), \qquad Q_{13}(z) = vQ_{11}(z) \tag{19a}$$

and

$$Q_{55}(z) = \frac{E(z)}{2(1+v)} \tag{19b}$$

3.4 Equations of motion

Hamilton's principle is used herein to derive the equations of motion. The principle can be stated in analytical form as (Thai and Choi 2012)

$$\int_{t_1}^{t_2} \left(\delta U + \delta U_{ef} + \delta V - \delta T\right)dt = 0 \tag{20}$$

Where t is the time; t_1 and t_2 are the initial and end time, respectively; δU is the virtual variation of the strain energy; δU_{ef} the potential energy of elastic foundation; δV is the variation of work done by external forces; and δT is the virtual variation of the kinetic energy. The variation of the strain energy of the beam can be stated as

$$\begin{aligned}
\delta U &= \int_0^L \int_{-\frac{h}{2}}^{\frac{h}{2}} (\sigma_x \delta\,\varepsilon_x + \sigma_z \delta\,\varepsilon_z + \tau_{xz}\delta\,\gamma_{xz})dzdx \\
&= \int_0^L \left(N_x\delta\varepsilon_x^0 + N_z\delta\varepsilon_z^0 - M_x^b\delta k_x^b - M_x^s\delta k_x^b + Q_{xz}\delta\gamma_{xz}^0\right)dx
\end{aligned} \tag{21}$$

Where N_x, M_x^b, M_x^s, N_z and Q_{xz} are the stress resultants defined as

$$(N_x, M_x^b, M_x^s) = \int_{-\frac{h}{2}}^{\frac{h}{2}} (1, z, f(z))\,\sigma_x dz \tag{22a}$$

$$N_z = \int_{-\frac{h}{2}}^{\frac{h}{2}} \sigma_z g^{'}(z)dz \tag{22b}$$

$$Q_{xz} = \int_{-\frac{h}{2}}^{\frac{h}{2}} \tau_{xz} g(z) dz \tag{22c}$$

The variation of the potential energy of elastic foundation given by

$$\delta U_{ef} = \int_0^L f_e \, \delta w_0 dx \tag{23}$$

where f_e is the density of reaction force of the foundation. For the Pasternak foundation model (Mantari *et al*. 2014)

$$f_e = K_w w_0 - K_p \frac{\partial^2 w_0}{\partial x^2} \tag{24}$$

If the foundation is modelled as the linear Winkler foundation, the coefficient K_p in Eq. (24) is zero. The variation of work done by externally transverse load q can be expressed as

$$\delta V = -\int_0^L q \delta w_0 dx \tag{28}$$

The variation of the kinetic energy can be expressed as

$$
\begin{aligned}
\delta T &= \int_0^L \int_{-\frac{h}{2}}^{\frac{h}{2}} \rho(z)[\dot{u}\delta\dot{u} + \dot{w}\delta\dot{w}] \, dzdx \\
&= \int_0^L \left\{ I_0[\dot{u}_0\delta\dot{u}_0 + \dot{w}_0\delta\dot{w}_0] + J_0(\dot{w}_0\delta\dot{\varphi}_z + \dot{\varphi}_z\delta\dot{w}_0) - I_1\left(\dot{u}_0\frac{\partial\delta\dot{w}_0}{\partial x} + \frac{\partial\dot{w}_0}{\partial x}\delta\dot{u}_0\right) \right. \\
&\quad + J_1\left((k_1A')\left(\dot{u}_0\frac{\partial\delta\dot{\theta}}{\partial x} + \frac{\partial\dot{\theta}}{\partial x}\delta\dot{u}_0\right)\right) + I_2\left(\frac{\partial\dot{w}_0}{\partial x}\frac{\partial\delta\dot{w}_0}{\partial x}\right) + K_2(k_1A')^2\left(\frac{\partial\dot{\theta}}{\partial x}\frac{\partial\delta\dot{\theta}}{\partial x}\right) \\
&\quad \left. - J_2\left((k_1A')\left(\frac{\partial\dot{w}_0}{\partial x}\frac{\partial\delta\dot{\theta}}{\partial x} + \frac{\partial\dot{\theta}}{\partial x}\frac{\partial\delta\dot{w}_0}{\partial x}\right)\right) + K_0\dot{\varphi}_z\delta\dot{\varphi}_z \right\} dx
\end{aligned}
\tag{26}
$$

Where an over dot designates the differentiation with respect to the time variable t; $\rho(z)$ is the mass density; and (I_i, J_i, K_i) are mass inertias expressed by

$$(I_0, I_1, I_2) = \int_{-h/2}^{h/2} (1, z, z^2)\rho(z)dz \tag{27a}$$

$$(J_1, J_2, K_2) = \int_{-h/2}^{h/2} (f, z\,f, f^2)\rho(z)dz \tag{27b}$$

$$(J_0, K_0) = \int_{-h/2}^{h/2} (g, g^2)\rho(z)dz \tag{27c}$$

Substituting the expressions for δU, δU_{ef}, δV and δT from Eqs. (21), (23), (25) and (26) into Eq. (20) and integrating the displacement gradients by parts and setting the coefficients of δu_0, δw_0, $\delta \theta$ and $\delta \varphi_z$ to zero separately, the following equations of motion are obtained

$$\delta u_0: \qquad \frac{\partial N_x}{\partial x} = I_0 \ddot{u}_0 - I_1 \frac{\partial \ddot{w}_0}{\partial x} + k_1 A' J_1 \frac{\partial \ddot{\theta}}{\partial x} \tag{28a}$$

$$\delta w_0: \qquad \frac{d^2 M_x^b}{dx^2} + q - f_e = I_0 \ddot{w}_0 + J_0 \ddot{\varphi}_z + I_1 \frac{\partial \ddot{u}_0}{\partial x} \\ - I_2 \frac{\partial^2 \ddot{w}_0}{\partial x^2} + J_2 k_1 A' \frac{\partial^2 \ddot{\theta}}{\partial x^2} \tag{28b}$$

$$\delta \theta: \qquad -k_1 M_x^s + k_1 A' \frac{\partial Q_{xz}}{\partial x} = -J_1 k_1 A' \frac{\partial \ddot{u}_0}{\partial x} \\ - K_2 (k_1 A')^2 \frac{\partial^2 \ddot{\theta}}{\partial x^2} + J_2 k_1 A' \frac{\partial^2 \ddot{w}_0}{\partial x^2} \tag{28c}$$

$$\delta \varphi_z: \qquad \frac{\partial Q_{xz}}{\partial x} - N_z = J_0 \ddot{w}_0 + K_0 \ddot{\varphi}_z \tag{28d}$$

Introducing Eq. (22) into Eq. (28), the equations of motion can be expressed in terms of displacements (u_0, w_0, θ, φ_z) and the appropriate equations take the form

$$A_{11} \frac{\partial^2 u_0}{\partial x^2} - B_{11} \frac{\partial^3 w_0}{\partial x^3} + B_{11}^s k_1 \frac{\partial \theta}{\partial x} + X_{13} \frac{\partial \varphi_z}{\partial x} \\ = I_0 \ddot{u}_0 - I_1 \frac{\partial \ddot{w}_0}{\partial x} + J_1 A' k_1 \frac{\partial \ddot{\theta}}{\partial x} \tag{29a}$$

$$B_{11} \frac{\partial^3 u_0}{\partial x^3} - D_{11} \frac{\partial^4 w_0}{\partial x^4} + D_{11}^s k_1 \frac{\partial^2 \theta}{\partial x^2} + Y_{13} \frac{\partial^2 \varphi_z}{\partial x^2} + q - K_w w_0 - K_p \frac{\partial^2 w_0}{\partial x^2} \\ = I_0 \ddot{w}_0 + J_0 \ddot{\varphi}_z + I_1 \frac{\partial \ddot{u}_0}{\partial x} - I_2 \frac{\partial^2 \ddot{w}_0}{\partial x^2} + J_2 k_1 A' \frac{\partial^2 \ddot{\theta}}{\partial x^2} \tag{29b}$$

$$-B_{11}^s k_1 \frac{\partial u_0}{\partial x} + D_{11}^s k_1 \frac{\partial^2 w_0}{\partial x^2} - H_{11}^s k_1^2 \theta + A_{55}^s (k_1 A')^2 \frac{\partial^2 \theta}{\partial x^2} - k_1 Y_{13}^s \varphi_z + k1 A' A_{55}^s \frac{\partial^2 \varphi_z}{\partial x^2} \\ = -J_1 k_1 A' \frac{\partial \ddot{u}_0}{\partial x} + J_2 k_1 A' \frac{\partial^2 \ddot{w}_0}{\partial x^2} - K_2 (k_1 A')^2 \frac{\partial^2 \ddot{\theta}}{\partial x^2} \tag{29c}$$

$$-X_{13} \frac{\partial u_0}{\partial x} + Y_{13} \frac{\partial^2 w_0}{\partial x^2} + \left(k_1(A_{55}^s - Y_{13}^s)\right)\theta + A_{55}^s \frac{\partial^2 \varphi_z}{\partial x^2} - Z_{33}\varphi_z \\ = J_0 \ddot{w}_0 + K_0 \ddot{\varphi}_z \tag{29d}$$

Where A_{11}, D_{11}, etc., are the beam stiffness, defined by

$$\left(A_{ij}, A_{ij}^s, B_{ij}, D_{ij}, B_{ij}^s, D_{ij}^s, H_{ij}^s\right) = \int_{-\frac{h}{2}}^{\frac{h}{2}} Q_{ij}(1, g^2(z), z, z^2, f(z), z\, f(z), f^2(z))dz \tag{30a}$$

$$\left(X_{ij}, Y_{ij}, B_{ij}^s, Y_{ij}^s, Z_{ij}\right) = \int_{-\frac{h}{2}}^{\frac{h}{2}} Q_{ij}\left(1, z, f(z), g'(z)g'(z)\right)dz \tag{30b}$$

3.5 Analytical solution

Navier-type analytical solutions are obtained for the bending and free vibration analysis of functionally graded beams resting on two parameter elastic foundation. According to the Navier-type solution technique, the unknown displacement variables are expanded in a Fourier series as given below

$$\begin{Bmatrix} u_0 \\ w_0 \\ \theta \\ \varphi_z \end{Bmatrix} = \sum_{m=1}^{\infty} \begin{Bmatrix} U_m \cos(\alpha x)\, e^{i\omega t} \\ W_m \sin(\alpha x)\, e^{i\omega t} \\ X_m \sin(\alpha x)\, e^{i\omega t} \\ \Phi_m \sin(\alpha x)\, e^{i\omega t} \end{Bmatrix} \tag{31}$$

Where (U_m, W_m, X_m, Φ_m) are unknown parameters to be determined and ω is the natural frequency. α is expressed as

$$\alpha = m\pi/L \tag{32}$$

The transverse load q is also expanded in Fourier series as

$$q(x) = \sum_{m=1,3,5}^{\infty} Q_m \sin \alpha x \tag{33}$$

Where Q_m is the load amplitude calculated from

$$Q_m = \frac{2}{L}\int_0^L q(x)\sin(\alpha x)dx \tag{34}$$

The coefficients Q_m are given below for some typical loads. For the case of a sinusoidally distributed load, we have

$$m = 1 \quad and \quad Q_1 = q_0 \tag{35a}$$

And for the case of uniform distributed load, we have

$$Q_m = \frac{4q_0}{m\pi}, \quad (m = 1,3,5\ldots) \tag{3b}$$

Substituting Eqs. (31) and (33) into Eq. (29), the analytical solutions can be obtained by the eigenvalue equations below, for any fixed value of m.

For free vibration problem

$$([K] - \omega^2[M])\{\Delta\} = \{0\} \tag{36}$$

For static problems, we obtain the following operator equation

$$[K]\{\Delta\} = \{F\} \tag{37}$$

Where

$$[K] = \begin{bmatrix} a_{11} & a_{12} & a_{13} & a_{14} \\ a_{12} & a_{22} & a_{23} & a_{24} \\ a_{13} & a_{23} & a_{33} & a_{34} \\ a_{14} & a_{24} & a_{34} & a_{44} \end{bmatrix}, \tag{38a}$$

$$[M] = \begin{bmatrix} m_{11} & m_{12} & m_{13} & m_{14} \\ m_{12} & m_{22} & m_{23} & m_{24} \\ m_{13} & m_{23} & m_{33} & m_{34} \\ m_{14} & m_{24} & m_{34} & m_{44} \end{bmatrix}, \tag{38b}$$

and

$$\{\Delta\} = \begin{Bmatrix} U_m \\ W_m \\ X_m \\ \Phi_m \end{Bmatrix}, \qquad \{\Delta\} = \begin{Bmatrix} 0 \\ Q_m \\ 0 \\ 0 \end{Bmatrix} \tag{38c}$$

With

$$\begin{aligned}
&a_{11} = A_{11}\alpha^2, \quad a_{12} = -B_{11}\alpha^3, \quad a_{13} = -B_{11}^s\alpha k_1, \quad a_{13} = -X_{13}\alpha, \\
&a_{22} = D_{11}\alpha^4 + K_w + K_p\alpha^2, \quad\quad a_{23} = D_{11}^s\alpha^2 k_1, \quad a_{24} = Y_{13}\alpha^2, \\
&a_{33} = H_{11}^s k_1^2 + A_{55}^s(k_1 A')^2\alpha^2, \quad\quad a_{34} = Y_{13}^s k_1 + A_{55}^s(k_1 A')\alpha^2
\end{aligned} \tag{39a}$$

$$\begin{aligned}
&m_{11} = I_0, \quad m_{12} = -I_1\alpha, \quad m_{13} = J_1\alpha k_1 A', \quad m_{14} = 0, \\
&m_{22} = I_0 + I_2\alpha^2, \quad\quad m_{23} = -J_2\alpha^2 k_1 A', \quad m_{24} = J_0, \\
&m_{33} = K_2\alpha^2(k_1 A')^2, \quad m_{34} = 0, \quad\quad m_{44} = K_0
\end{aligned} \tag{39b}$$

4. Numerical results and discussions

Numerical results for displacements, stresses and natural frequencies of functionally graded beams resting on two parameter elastic foundation are presented in this section to verify the accuracy of the present formulation. The beam is made of the following material properties:

Ceramic: Alumina (Al_2O_3): $E_c = 380$ GPa; $\nu = 0.3$; $\rho_c = 3960$ kg/m³.
Metal: Aluminium (Al): $E_m = 70$ GPa; $\nu = 0.3$; $\rho_m = 2702$ kg/m³.

For simplicity, the following non-dimensional parameters are used:

Axial displacement: $\overline{u} = 100 \frac{E_m h^3}{q_0 L^4} u\left(0, -\frac{h}{2}\right)$;

Transverse displacement: $\overline{w} = 100 \frac{E_m h^3}{q_0 L^4} w\left(\frac{L}{2}, 0\right)$;

Axial stress: $\overline{\sigma}_x = \frac{h}{q_0 L} \sigma_x\left(\frac{L}{2}, \frac{h}{2}\right)$;

Transverse shear stress: $\overline{\tau}_{xz} = \frac{h}{q_0 L} \tau_{xz}(0, 0)$;

Fundamental frequency: $\overline{\omega} = \frac{\omega L^2}{h} \sqrt{\frac{\rho_m}{E_m}}$;

Finally, the non-dimensional elastic foundation parameters are: $\xi_w = \frac{K_w l^2}{E_m h}$, $\xi_p = \frac{K_p}{E_m h}$.

Study 1: Bending and free vibration of functionally graded beams on elastic foundations

In this example, the bending and free vibration responses of FG beam under sinusoidal load is investigated. Displacements and stresses obtained by using the present hyperbolic beam theory (HBT), the second quasi-3D hyperbolic beam theory of Mechab *et al.* (2017), the inverse hyperbolic theory (IHBT) of Sayyad and Ghugal (2018), the parabolic beam theory (PBT) of Reddy (1984) and first order beam theory (FBT) of Timoshenko (1921) are presented in Tables 1, 2 and 3. These results are obtained for $L/h = 5$ and $L/h = 20$ and various values of power law index (p) and with foundation parameters (ξ_w, ξ_p). It is seen that the displacements and stresses obtained from the two present theory are in excellent agreement with those obtained from Sayyad and Ghugal (2018) and PBT. On the contrary, the FBT underestimates the displacements and stresses. Furthermore, it is observed from the Tables 1, 2 and 3 that the displacements increase with the increase in power-law index whereas stresses are identical when beam is made of fully ceramic $(p = 0)$ or fully metal $(p = \infty)$. This is due to the fact that an increase of the power-law index makes FG beams more flexible i.e., reduces their stiffness. It is also observed from Tables 1, 2 and 3 that the displacement and stresses of FG beam are reduced when it is resting on two

Table 1 Non-dimensional displacements and stresses of functionally graded beam subjected to sinusoidal load ($\xi_w = 0$ and $\xi_p = 0$)

p	Theory	$L/h = 5$				$L/h = 20$			
		$\overline{u}$	$\bar{w}$	$\bar{\sigma}_x$	$\bar{\tau}_{xz}$	$\overline{u}$	$\bar{w}$	$\bar{\sigma}_x$	$\bar{\tau}_{xz}$
0	**Present $(\varepsilon_z \neq 0)$**	**0.7254**	**2.5007**	**3.1282**	**0.4877**	**0.1784**	**2.2839**	**12.180**	**0.4884**
	Mechab *et al.* (2017)	**0.7242**	**2.5011**	**3.1318**	**0.4641**	**0.1784**	**2.2839**	**12.181**	**0.4645**
	Sayyad and Ghugal (2018)	0.7253	2.5019	3.0922	0.4800	0.1784	2.2839	12.171	0.4806
	Reddy (1984)	0.7251	2.5020	3.0916	0.4769	0.1784	2.2838	12.171	0.4774
	Timoshenko (1921)	0.7129	2.0523	3.0396	0.2653	0.1782	2.2839	12.158	0.2653
1	**Present $(\varepsilon_z \neq 0)$**	**1.7798**	**4.9437**	**4.8475**	**0.4877**	**0.4400**	**4.5774**	**18.828**	**0.4884**
	Mechab *et al.* (2017)	**1.7778**	**4.9442**	**4.8537**	**0.4641**	**0.4399**	**4.5774**	**18.829**	**0.4645**
	Sayyad and Ghugal (2018)	1.7796	4.9441	4.7867	0.5248	0.4400	4.5774	18.814	0.5245
	Reddy (1984)	1.7793	4.9458	4.7857	0.5243	0.4400	4.5773	18.813	0.5249
	Timoshenko (1921)	1.7588	4.8807	4.6979	0.5376	0.4397	4.5734	18.792	0.5376

Table 1 Non-dimensional displacements and stresses of functionally graded beam subjected to sinusoidal load ($\xi_w = 0$ and $\xi_p = 0$)

p	Theory	$L/h = 5$				$L/h = 20$			
		$\bar{u}$	$\bar{w}$	$\bar{\sigma}_x$	$\bar{\tau}_{xz}$	$\bar{u}$	$\bar{w}$	$\bar{\sigma}_x$	$\bar{\tau}_{xz}$
5	**Present ($\varepsilon_z \neq 0$)**	**2.8656**	**7.7748**	**6.6968**	**0.3980**	**0.7069**	**6.9543**	**25.816**	**0.3988**
	Mechab *et al.* (2017)	**2.8615**	**7.7625**	**6.6919**	**0.3713**	**0.7068**	**6.9535**	**25.815**	**0.3718**
	Sayyad and Ghugal (2018)	2.8649	7.7739	6.6079	0.5274	0.7069	6.9541	25.795	0.5313
	Reddy (1984)	2.8644	7.7723	6.6057	0.5314	0.7069	6.9540	25.794	0.5323
	Timoshenko (1921)	2.8250	7.5056	6.4382	0.9942	0.7062	6.9373	25.752	0.9942
10	**Present ($\varepsilon_z \neq 0$)**	**3.0004**	**8.6522**	**8.0174**	**0.4344**	**0.7380**	**7.6422**	**30.948**	**0.4352**
	Mechab *et al.* (2017)	**2.9954**	**8.6453**	**8.0119**	**0.4082**	**0.7379**	**7.6417**	**30.948**	**0.4088**
	Sayyad and Ghugal (2018)	2.9995	8.6539	7.9102	0.4237	0.7380	7.6422	30.923	0.4263
	Reddy (1984)	2.9989	8.6530	7.9080	0.4226	0.7379	7.6421	30.999	0.4233
	Timoshenko (1921)	2.9488	8.3259	7.7189	1.2320	0.7372	7.6215	30.875	1.2320
∞	**Present ($\varepsilon_z \neq 0$)**	**3.9379**	**13.576**	**3.1282**	**0.4877**	**0.9686**	**12.398**	**12.180**	**0.4884**
	Mechab *et al.* (2017)	**3.9315**	**13.577**	**3.1318**	**0.4641**	**0.9685**	**12.398**	**12.181**	**0.4645**
	Sayyad and Ghugal (2018)	3.9371	13.582	3.0922	0.4800	0.9677	12.329	12.171	0.4806
	Reddy (1984)	3.9363	13.582	3.0916	0.4769	0.9686	12.398	12.171	0.4774
	Timoshenko (1921)	3.8702	12.552	3.0396	0.3183	0.9676	12.398	12.158	0.3183

Table 2 Non-dimensional displacements and stresses of functionally graded beam resting on two parameter elastic foundation and subjected to sinusoidal load ($\xi_w = 0.1$ and $\xi_p = 0$)

p	Theory	$L/h = 5$				$L/h = 20$			
		$\bar{u}$	$\bar{w}$	$\bar{\sigma}_x$	$\bar{\tau}_{xz}$	$\bar{u}$	$\bar{w}$	$\bar{\sigma}_x$	$\bar{\tau}_{xz}$
0	**Present ($\varepsilon_z \neq 0$)**	**0.6826**	**2.3534**	**2.9438**	**0.4590**	**0.0932**	**1.1935**	**6.3652**	**0.2552**
	Mechab *et al.* (2017)	**0.6815**	**2.3536**	**2.9473**	**0.4367**	**0.0932**	**1.1935**	**6.3657**	**0.2428**
	Sayyad and Ghugal (2018)	0.6826	2.3547	2.9102	0.4517	0.0932	1.1935	6.3608	0.2511
	Reddy (1984)	0.6824	2.3547	2.9096	0.4488	0.0932	1.1935	6.3606	0.2495
	Timoshenko (1921)	0.6716	2.3205	2.8607	0.2499	0.0932	1.1929	6.3539	0.1387
1	**Present ($\varepsilon_z \neq 0$)**	**1.5838**	**4.3992**	**4.3135**	**0.4341**	**0.1554**	**1.6169**	**6.6508**	**0.1725**
	Mechab *et al.* (2017)	**1.5820**	**4.3996**	**4.3191**	**0.4129**	**0.1554**	**1.6169**	**6.6513**	**0.1641**
	Sayyad and Ghugal (2018)	1.5838	4.4015	4.2600	0.4657	0.1554	1.6169	6.6458	0.1851
	Reddy (1984)	1.5835	4.4015	4.2591	0.4666	0.1554	1.6169	6.6456	0.1854
	Timoshenko (1921)	1.5675	4.3499	4.1871	0.4791	0.1554	1.6164	6.6418	0.1900
5	**Present ($\varepsilon_z \neq 0$)**	**2.3987**	**6.5080**	**5.6056**	**0.3332**	**0.1869**	**1.8389**	**6.8265**	**0.1054**
	Mechab *et al.* (2017)	**2.3959**	**6.4996**	**5.6032**	**0.3109**	**0.1869**	**1.8389**	**6.8268**	**0.0983**
	Sayyad and Ghugal (2018)	2.3987	6.5089	5.5327	0.4416	0.1869	1.8389	6.8212	0.1397
	Reddy (1984)	2.3984	6.5078	5.5310	0.4450	0.1869	1.8389	6.8211	0.1408
	Timoshenko (1921)	2.3786	6.3198	5.4210	0.8371	0.1871	1.8377	6.8221	0.2634

Table 2 Non-dimensional displacements and stresses of functionally graded beam resting on two parameter elastic foundation and subjected to sinusoidal load ($\xi_w = 0.1$ and $\xi_p = 0$)

p	Theory	$L/h = 5$				$L/h = 20$			
		$\bar{u}$	$\bar{w}$	$\bar{\sigma}_x$	$\bar{\tau}_{xz}$	$\bar{u}$	$\bar{w}$	$\bar{\sigma}_x$	$\bar{\tau}_{xz}$
	Present ($\varepsilon_z \neq 0$)	**2.4662**	**7.1115**	**6.5898**	**0.3570**	**0.1819**	**1.8838**	**7.6286**	**0.1072**
	Mechab *et al*. (2017)	**2.4625**	**7.1072**	**6.5866**	**0.3356**	**0.1819**	**1.8837**	**7.6287**	**0.1008**
10	Sayyad and Ghugal (2018)	2.4659	7.1147	6.5033	0.3484	0.1819	1.8838	7.6225	0.1051
	Reddy (1984)	2.4655	7.1141	6.5016	0.3474	0.1819	1.8838	7.5606	0.1043
	Timoshenko (1921)	2.4408	6.8914	6.3891	1.0197	0.1821	1.8825	7.6262	0.3043
	Present ($\varepsilon_z \neq 0$)	**2.9387**	**10.131**	**2.3344**	**0.3640**	**0.1625**	**2.0805**	**2.0438**	**0.0819**
	Mechab *et al*. (2017)	**2.9339**	**10.132**	**2.3372**	**0.3463**	**0.1625**	**2.0805**	**2.0441**	**0.0779**
∞	Sayyad and Ghugal (2018)	2.9391	10.139	2.3084	0.3583	0.1631	2.0785	2.0425	0.0806
	Reddy (1984)	2.9385	10.139	2.3079	0.3560	0.1625	2.0805	2.0424	0.0801
	Timoshenko (1921)	2.8891	10.140	2.2691	0.2376	0.1624	2.0805	2.0403	0.0534

Table 3 Non-dimensional displacements and stresses of functionally graded beam resting on two parameter elastic foundation and subjected to sinusoidal load ($\xi_w = 0.1$ and $\xi_p = 0.1$)

p	Theory	$L/h = 5$				$L/h = 20$			
		$\bar{u}$	$\bar{w}$	$\bar{\sigma}_x$	$\bar{\tau}_{xz}$	$\bar{u}$	$\bar{w}$	$\bar{\sigma}_x$	$\bar{\tau}_{xz}$
	Present ($\varepsilon_z \neq 0$)	**0.4316**	**1.4878**	**1.8611**	**0.2902**	**0.0163**	**0.2089**	**1.1143**	**0.0446**
	Mechab *et al*. (2017)	**0.4309**	**1.4880**	**1.8634**	**0.2761**	**0.0163**	**0.2089**	**1.1144**	**0.0425**
0	Sayyad and Ghugal (2018)	0.4317	1.4894	1.8407	0.2857	0.0163	0.2090	1.1136	0.0440
	Reddy (1984)	0.4316	1.4894	1.8403	0.2839	0.0163	0.2090	1.1136	0.0437
	Timoshenko (1921)	0.4271	1.4756	1.8093	0.1589	0.0163	0.2089	1.1124	0.0243
	Present ($\varepsilon_z \neq 0$)	**0.7588**	**2.1077**	**2.0667**	**0.2079**	**0.0211**	**0.2189**	**0.9007**	**0.0234**
	Mechab *et al*. (2017)	**0.7579**	**2.1079**	**2.0694**	**0.1979**	**0.0211**	**0.2189**	**0.9008**	**0.0222**
1	Sayyad and Ghugal (2018)	0.7592	2.1100	2.0422	0.2232	0.0211	0.2190	0.9001	0.0251
	Reddy (1984)	0.7591	2.1100	2.0417	0.2237	0.0211	0.2190	0.9001	0.0251
	Timoshenko (1921)	0.7560	2.0981	2.0195	0.2311	0.0211	0.2190	0.8998	0.0257
	Present ($\varepsilon_z \neq 0$)	**0.9197**	**2.4953**	**2.1493**	**0.1277**	**0.0226**	**0.2226**	**0.8264**	**0.0128**
	Mechab *et al*. (2017)	**0.9195**	**2.4944**	**2.1504**	**0.1193**	**0.0226**	**0.2226**	**0.8265**	**0.0119**
5	Sayyad and Ghugal (2018)	0.9205	2.4976	2.1231	0.1694	0.0226	0.2226	0.8258	0.0170
	Reddy (1984)	0.9204	2.4975	2.1226	0.1708	0.0226	0.2226	0.8258	0.0170
	Timoshenko (1921)	0.9294	2.4693	2.1181	0.3271	0.0227	0.2226	0.8264	0.0319
	Present ($\varepsilon_z \neq 0$)	**0.8944**	**2.5790**	**2.3898**	**0.1294**	**0.0216**	**0.2233**	**0.9042**	**0.0127**
	Mechab *et al*. (2017)	**0.8935**	**2.5789**	**2.3900**	**0.1218**	**0.0216**	**0.2233**	**0.9042**	**0.0119**
10	Sayyad and Ghugal (2018)	0.8950	2.5820	2.3601	0.1264	0.0216	0.2233	0.9035	0.0125
	Reddy (1984)	0.8948	2.5819	2.3596	0.1261	0.0215	0.2233	0.8934	0.0124
	Timoshenko (1921)	0.9039	2.5520	2.3660	0.3776	0.0216	0.2233	0.9045	0.0361

Table 3 Non-dimensional displacements and stresses of functionally graded beam resting on two parameter elastic foundation and subjected to sinusoidal load ($\xi_w = 0.1$ and $\xi_p = 0.1$)

p	Theory	$L/h = 5$				$L/h = 20$			
		$\bar{u}$	$\bar{w}$	$\bar{\sigma}_x$	$\bar{\tau}_{xz}$	$\bar{u}$	$\bar{w}$	$\bar{\sigma}_x$	$\bar{\tau}_{xz}$
	Present ($\varepsilon_z \neq 0$)	**0.8386**	**2.8910**	**0.6661**	**0.1038**	**0.0176**	**0.2258**	**0.2218**	**0.0088**
	Mechab *et al.* (2017)	**0.8373**	**2.8915**	**0.6669**	**0.0988**	**0.0176**	**0.2258**	**0.2218**	**0.0085**
∞	Sayyad and Ghugal (2018)	0.8393	2.8955	0.6592	0.1023	0.0177	0.2258	0.2217	0.0088
	Reddy (1984)	0.8392	2.8955	0.6591	0.1017	0.0176	0.2258	0.2217	0.0087
	Timoshenko (1921)	0.8250	2.8955	0.6479	0.0679	0.0176	0.2258	0.2214	0.0058
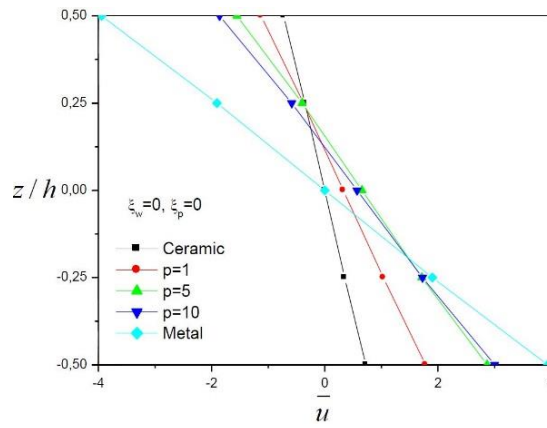
Fig. 5 Non-dimensional axial displacement through the thickness (L/h = 5, non dimensional elastic foundation parameters are: $\xi_w = \xi_p = 0$)
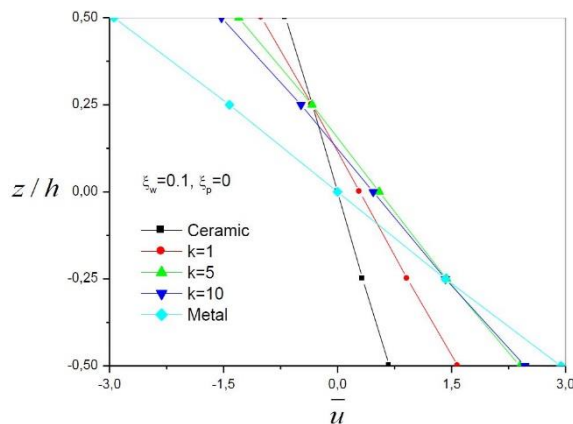
Fig. 6 Non-dimensional axial displacement through the thickness (L/h = 5, non-dimensional elastic foundation parameters are : $\xi_w = 0.1$ and $\xi_p = 0$)
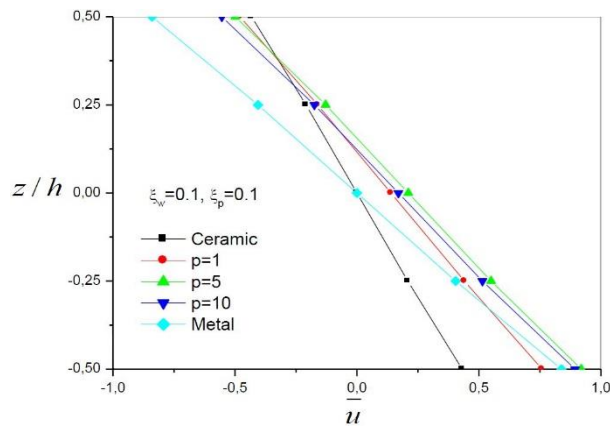
Fig. 7 Non-dimensional axial displacement through the thickness (L/h = 5, non-dimensional elastic foundation parameters are : $\xi_w = 0.1$ and $\xi_p = 0.1$)
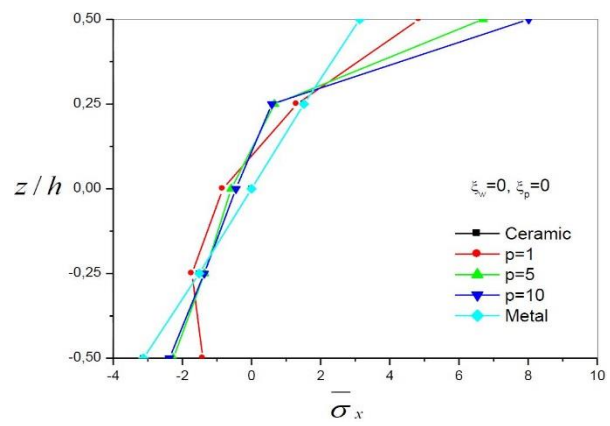

Fig. 8 Non-dimensional axial stress through the thickness (L/h = 5, non-dimensional elastic foundation parameters are : $\xi_w = 0$ and $\xi_p = 0$)
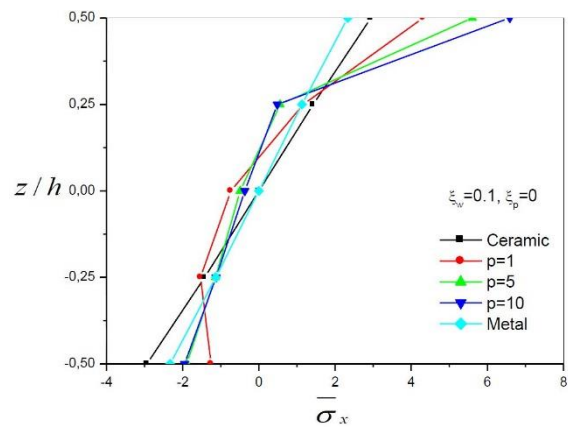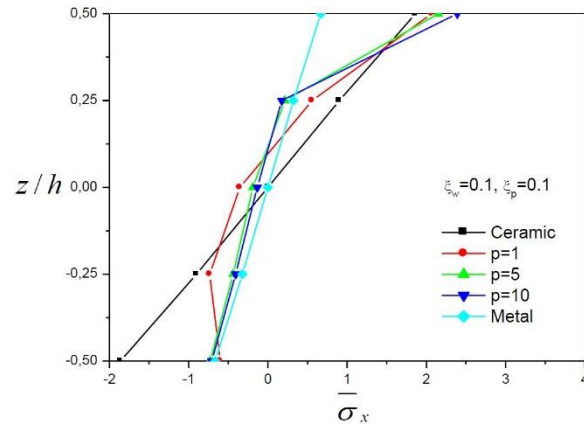

Fig. 9 Non-dimensional axial stress through the thickness (L/h = 5, non-dimensional elastic foundation parameters are : $\xi_w = 0.1$ and $\xi_p = 0$)

Fig. 10 Non-dimensional axial stress through the thickness (L/h = 5, non-dimensional elastic foundation parameters are : $\xi_w = 0.1$ and $\xi_p = 0.1$)

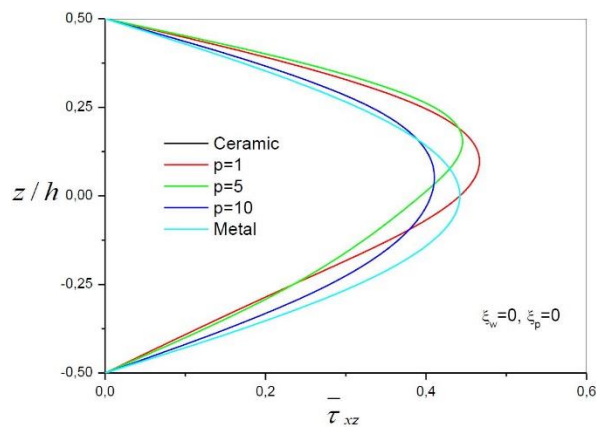

Fig. 11 Non-dimensional transverse shear stress through the thickness (L/h = 5, non-dimensional elastic foundation parameters are : $\xi_w = 0$ and $\xi_p = 0$)

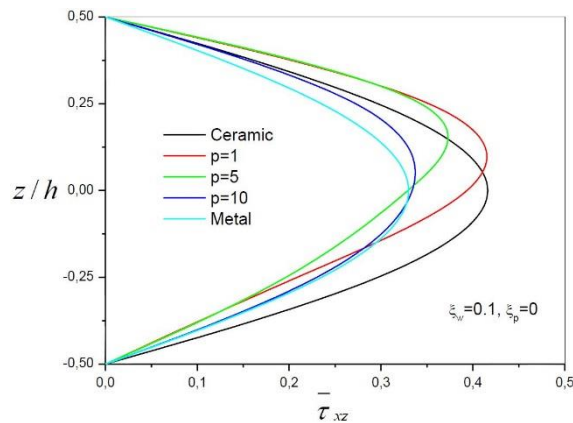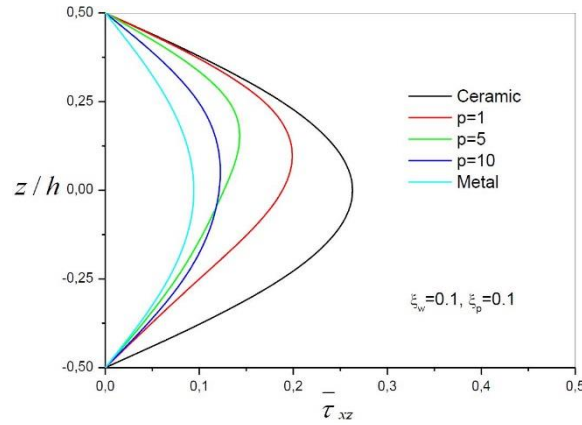Fig. 12 Non-dimensional transverse shear stress through the thickness (L/h = 5, non-dimensional elastic foundation parameters are : $\xi_w = 0.1$ and $\xi_p = 0$)

Fig. 13 Non-dimensional transverse shear stress through the thickness (L/h = 5, non-dimensional elastic foundation parameters are : $\xi_w = 0.1$ and $\xi_p = 0.1$)

parameter elastic foundation i.e., Winkler layer and shearing layer.

Figs. 5-7 show effect of power-law index and foundation parameter on axial displacement of FG beam subjected to sinusoidal load using the present hyperbolic beam theory (HBT). Figs. 8-10 show non-linear variation of bending stress for $p = 5$ and 10 and linear variation for $p = 0$ and ∞. Through-the-thickness variations of transverse shear stresses are shown in Figs. 11-13 for various values of power law index and foundation parameters.

The non-dimensional natural frequencies of a FG beam resting on two parameters elastic foundation obtained from the present the present hyperbolic beam (HBT) and the second hyperbolic beam theory of Mechab *et al.* (2017), are given in Tables 4 and 5 for different values of power-law index. The present results are compared with those presented by Sayyad and Ghugal (2018). The examination of Tables 4 and 5 reveals that the fundamental frequencies obtained using the two present theories are in excellent agreement with the previously published results. It is observed that an increase in the value of the p index leads to a reduction of fundamental

Table 4 Non-dimensional flexural natural frequencies of functionally graded beams resting on elastic foundation $(L/h = 5)$

					p					
L/h	Mode	ξ_w	ξ_p	Theory	0	1	2	5	10	∞
				Present $(\varepsilon_z \neq 0)$	**5.1528**	**3.9904**	**3.6262**	**3.4001**	**3.2811**	**2.6773**
		0	0	Mechab *et al.* (2017)	**5.1528**	**3.9904**	**3.6268**	**3.4028**	**3.2825**	**2.6773**
				Sayyad and Ghugal (2018)	5.1453	3.9826	3.6184	3.3917	3.2727	2.6734
				Present $(\varepsilon_z \neq 0)$	**5.3115**	**4.2300**	**3.9045**	**3.7159**	**3.6187**	**3.0987**
5	1	0.1	0	Mechab *et al.* (2017)	**5.3116**	**4.2299**	**3.9051**	**3.7183**	**3.6199**	**3.0987**
				Sayyad and Ghugal (2018)	5.3038	4.2216	3.8961	3.7066	3.6094	3.0942
				Present $(\varepsilon_z \neq 0)$	**6.6780**	**6.1073**	**5.9913**	**5.9949**	**6.0020**	**5.7904**
		0.1	0.1	Mechab *et al.* (2017)	**6.6779**	**6.1073**	**5.9916**	**5.9964**	**6.0030**	**5.7904**
				Sayyad and Ghugal (2018)	6.6689	6.0973	5.9810	5.9830	5.9909	5.7903

Table 4 Non-dimensional flexural natural frequencies of functionally graded beams resting on elastic foundation $(L/h = 5)$

							p				
L/h	Mode	ξ_w	ξ_p	Theory	0	1	2	5	10	∞
5	2	0	0	**Present $(\varepsilon_z \neq 0)$**	**17.880**	**14.009**	**12.638**	**11.533**	**11.020**	**9.2905**
				Mechab *et al.* (2017)	**17.878**	**14.008**	**12.642**	**11.555**	**11.029**	**9.2895**
				Sayyad and Ghugal (2018)	17.589	13.754	12.388	11.260	10.748	9.1392
		0.1	0	**Present $(\varepsilon_z \neq 0)$**	**17.925**	**14.076**	**12.717**	**11.626**	**11.121**	**9.4159**
				Mechab *et al.* (2017)	**17.923**	**14.075**	**12.721**	**11.648**	**11.131**	**9.4149**
				Sayyad and Ghugal (2018)	17.633	13.820	12.465	11.351	10.848	9.2623
		0.1	0.1	**Present $(\varepsilon_z \neq 0)$**	**19.605**	**16.490**	**15.489**	**14.820**	**14.552**	**13.411**
				Mechab *et al.* (2017)	**19.603**	**16.489**	**15.491**	**14.836**	**14.559**	**13.409**
				Sayyad and Ghugal (2018)	19.287	16.200	15.200	14.493	14.224	13.240
	3	0	0	**Present $(\varepsilon_z \neq 0)$**	**34.198**	**27.091**	**24.307**	**21.689**	**20.546**	**17.769**
				Mechab *et al.* (2017)	**34.184**	**27.081**	**24.310**	**21.740**	**20.562**	**17.762**
				Sayyad and Ghugal (2018)	32.324	25.538	22.812	20.117	19.003	16.794
		0.1	0	**Present $(\varepsilon_z \neq 0)$**	**34.222**	**27.125**	**24.347**	**21.738**	**20.601**	**17.834**
				Mechab *et al.* (2017)	**34.207**	**27.115**	**24.349**	**21.788**	**20.617**	**17.827**
				Sayyad and Ghugal (2018)	32.346	25.570	22.849	20.163	19.053	16.855
		0.1	0.1	**Present $(\varepsilon_z \neq 0)$**	**36.209**	**29.948**	**27.621**	**25.663**	**24.889**	**22.747**
				Mechab *et al.* (2017)	**36.193**	**29.936**	**27.619**	**25.699**	**24.901**	**22.736**
				Sayyad and Ghugal (2018)	34.223	28.261	25.980	23.881	23.1.7	21.626

frequencies. This is due to the fact that an increase in the p-value results in a decrease in the value of the elastic modulus. Also, it is observed that the natural frequencies are increased when beam is resting on two parameters elastic foundation.

Table 5 Non-dimensional flexural natural frequencies of functionally graded beams resting on elastic foundation $(L/h = 20)$

							p				
L/h	Mode	ξ_w	ξ_p	Theory	0	1	2	5	10	∞
20	1	0	0	**Present $(\varepsilon_z \neq 0)$**	**5.4603**	**4.2050**	**3.8361**	**3.6484**	**3.5389**	**2.8371**
				Mechab *et al.* (2017)	**5.4603**	**4.2050**	**3.8361**	**3.6486**	**3.5391**	**2.8371**
				Sayyad and Ghugal (2018)	5.4603	4.2050	3.8361	3.6484	3.5389	2.8371
		0.1	0	**Present $(\varepsilon_z \neq 0)$**	**7.5533**	**7.0752**	**7.0185**	**7.0948**	**7.1280**	**6.9259**
				Mechab *et al.* (2017)	**7.5533**	**7.0752**	**7.0185**	**7.0950**	**7.1281**	**6.9259**
				Sayyad and Ghugal (2018)	7.5533	7.0751	7.0184	7.0948	7.1279	6.9259

Table 5 Non-dimensional flexural natural frequencies of functionally graded beams resting on elastic foundation $(L/h = 20)$

							p			
L/h	Mode	ξ_w	ξ_p	Theory	0	1	2	5	10	∞
				Present $(\varepsilon_z \neq 0)$	**18.052**	**19.224**	**19.752**	**20.389**	**20.703**	**21.020**
		0.1	0.1	**Mechab** *et al.* (2017)	**18.052**	**19.224**	**19.752**	**20.389**	**20.703**	**21.020**
				Sayyad and Ghugal (2018)	18.052	19.224	19.752	20.390	20.703	21.022
				Present $(\varepsilon_z \neq 0)$	**21.573**	**16.634**	**15.161**	**14.373**	**13.925**	**11.209**
		0	0	**Mechab** *et al.* (2017)	**21.573**	**16.634**	**15.162**	**14.376**	**13.927**	**11.209**
				Sayyad and Ghugal (2018)	21.571	16.631	15.158	14.370	13.922	11.208
	2			**Present** $(\varepsilon_z \neq 0)$	**22.192**	**17.575**	**16.254**	**15.599**	**15.230**	**12.858**
		0.1	0	**Mechab** *et al.* (2017)	**22.192**	**17.575**	**16.254**	**15.603**	**15.232**	**12.858**
				Sayyad and Ghugal (2018)	22.189	17.571	16.250	15.596	15.226	12.857
				Present $(\varepsilon_z \neq 0)$	**39.515**	**39.733**	**40.226**	**41.161**	**41.625**	**41.604**
		0.1	0.1	**Mechab** *et al.* (2017)	**39.515**	**39.733**	**40.227**	**41.162**	**41.626**	**41.604**
				Sayyad and Ghugal (2018)	39.513	39.730	40.223	41.157	41.624	41.615
				Present $(\varepsilon_z \neq 0)$	**47.593**	**36.768**	**33.467**	**31.571**	**30.534**	**24.729**
		0	0	**Mechab** *et al.* (2017)	**47.593**	**36.768**	**33.471**	**31.587**	**30.542**	**24.729**
				Sayyad and Ghugal (2018)	47.569	36.740	33.440	31.543	30.505	24.716
	3			**Present** $(\varepsilon_z \neq 0)$	**47.874**	**37.199**	**33.971**	**32.142**	**31.144**	**25.512**
		0.1	0	**Mechab** *et al.* (2017)	**47.874**	**37.199**	**33.974**	**32.158**	**31.153**	**25.512**
				Sayyad and Ghugal (2018)	47.851	37.171	33.943	32.114	31.116	25.499
				Present $(\varepsilon_z \neq 0)$	**68.383**	**64.908**	**64.560**	**65.287**	**65.669**	**64.339**
		0.1	0.1	**Mechab** *et al.* (2017)	**68.383**	**64.908**	**64.562**	**65.294**	**65.674**	**64.339**
				Sayyad and Ghugal (2018)	68.353	64.871	64.523	65.245	65.633	64.358

Study 2: Effect of micromechanical models on bending and free vibration analysis of FG beams

The effect of micromechanical models on bending and free vibration analysis of FG beams using the present hyperbolic beam theory (HBT) is presented for investigation. The results are presented in Tables 6 and 7 for FG beam with power law index $p = 2$ and two values of L/h. Effective Young's modulus is calculated using the aforementioned five micromechanical models. The results are given in terms of displacements and the various stresses. The results of the present hyperbolic beam theory (HBT) is compared with those presented by Zouatnia and Hadji (2019) with $(\varepsilon_z = 0)$. It can be observed that there is a good agreement between displacements and stresses using the different micromechanical models under sinusoidal load. The slight difference may be explained by the way that the Young's modulus is calculated. In addition, the use of the Reuss model leads to the highest displacement values, compared to other models, while that of Voigt's one implies the lowest values. The Reuss and Tamura models lead to almost the same results.

In Fig. 14, we present the variation of the axial stress $\overline{\sigma}_x$ through the thickness for different

Table 6 Non-dimensional displacements and stresses of functionally graded (P-FGM) beams
        (p = 2 and L = 5 h)

Theory		Sinusoidal load			
		$\bar{w}$	$\bar{u}$	$\bar{\sigma}_x$	$\bar{\tau}_{xz}$
Present $(\varepsilon_z \neq 0)$	**Voigt**	**6.3738**	**2.4053**	**5.6729**	**0.4482**
Zouatnia and Hadji (2019)	Voigt	6.3759	2.4058	5.6056	0.4482
Present $(\varepsilon_z \neq 0)$	**Reuss**	**8.0170**	**2.8658**	**7.3747**	**0.4347**
Zouatnia and Hadji (2019)	Reuss	8.0200	2.8664	7.2829	0.4347
Present $(\varepsilon_z \neq 0)$	**LRVE**	**7.3755**	**2.7336**	**6.4843**	**0.4223**
Zouatnia and Hadji (2019)	LRVE	7.3780	2.7341	6.4049	0.4223
Present $(\varepsilon_z \neq 0)$	**Tamura (q = 0)**	**8.0171**	**2.8658**	**7.3747**	**0.4347**
Zouatnia and Hadji (2019)	Tamura (q = 0)	8.0200	2.8664	7.2829	0.4347
Present $(\varepsilon_z \neq 0)$	**Tamura (q = 100)**	**7.3501**	**2.7094**	**6.5452**	**0.4303**
Zouatnia and Hadji (2019)	Tamura (q = 100)	7.3527	2.7100	6.4650	0.4302
Present $(\varepsilon_z \neq 0)$	**Mori-Tanaka**	**7.7979**	**2.8176**	**7.0819**	**0.4324**
Zouatnia and Hadji (2019)	Mori-Tanaka	7.8007	2.8183	6.9941	0.4323

Table 7 Non-dimensional displacements and stresses of functionally graded (P-FGM) beams
        (p = 2 and L = 20 h)

Theory		Sinusoidal load			
		$\bar{w}$	$\bar{u}$	$\bar{\sigma}_x$	$\bar{\tau}_{xz}$
Present $(\varepsilon_z \neq 0)$	**Voigt**	**5.8685**	**0.5952**	**21.9883**	**0.4489**
Zouatnia and Hadji (2019)	Voigt	5.8684	0.5952	21.9725	0.4489
Present $(\varepsilon_z \neq 0)$	**Reuss**	**7.2036**	**0.7067**	**28.5036**	**0.4355**
Zouatnia and Hadji (2019)	Reuss	7.2036	0.7067	28.4820	0.4355
Present $(\varepsilon_z \neq 0)$	**LRVE**	**6.6746**	**0.6751**	**25.0558**	**0.4231**
Zouatnia and Hadji (2019)	LRVE	6.6746	0.6751	25.0372	0.4231
Present $(\varepsilon_z \neq 0)$	**Tamura (q = 0)**	**7.2036**	**0.7067**	**28.5036**	**0.4355**
Zouatnia and Hadji (2019)	Tamura (q = 0)	7.2036	0.7067	28.4820	0.4355
Present $(\varepsilon_z \neq 0)$	**Tamura (q = 100)**	**6.6589**	**0.6691**	**25.3037**	**0.4310**
Zouatnia and Hadji (2019)	Tamura (q = 100)	6.6589	0.6691	25.2848	0.4310
Present $(\varepsilon_z \neq 0)$	**Mori-Tanaka**	**7.0222**	**0.6952**	**27.3700**	**0.4331**
Zouatnia and Hadji (2019)	Mori-Tanaka	7.0222	0.6952	27.3493	0.4331

micromechanical models. From this figure, it can be seen that all models give almost the same results in terms of axial stress except that of Voigt, which gives minimum tensile stresses at the top, and minimum compressive stresses at the bottom surface.

The effect of the micromechanical models on the variation of the transverse shear stress $\bar{\tau}_{xz}$ across the thickness is shown in Fig. 15. The Voigt model is the one, which gives the highest stresses compared with the others where the difference between the max stresses is minimal.
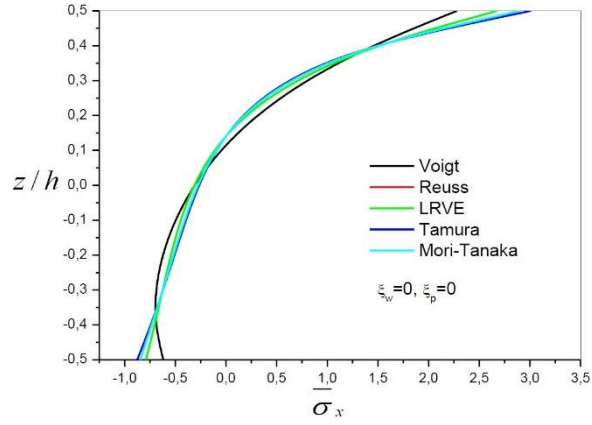
Fig. 14 Variation of the axial stress $\overline{\sigma}_x$ through-the-thickness of a FG beam for different micromechanical models ($L/h = 2$, $p = 1$)
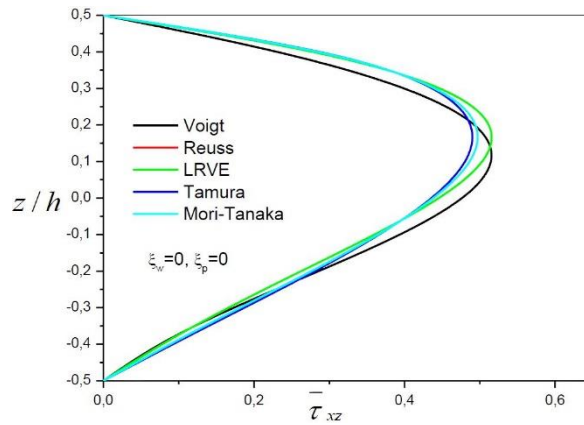

Fig. 15 Variation of the transverse shear stress $\overline{\tau}_{xz}$ through-the-thickness of a FG beam for different micromechanical models ($L/h = 2$, $p = 1$)

Table 8 Variation of fundamental frequency $\overline{\omega}$ with the power-law index p for FG beam

L/h	Theory		p					
			0	0.5	1	2	5	10
5	Ould Larbi *et al.* (2013)		5.1529	4.4108	3.9905	3.6263	3.4001	3.2812
	TBT (Simsek 2010)		5.1527	4.4111	3.9904	3.6264	3.4012	3.2816
	Present ($\varepsilon_z \neq 0$)	**Voigt**	5.1528	4.4107	3.9905	3.6263	3.4001	3.2811
		Reuss	5.1528	3.6231	3.3819	3.2381	3.1071	2.9951
		LRVE	5.1528	3.9096	3.5729	3.3731	3.2309	3.1071
		Tamura (q = 0)	5.1528	3.6231	3.3819	3.2381	3.1071	2.9951
		(q = 100)	5.1528	3.9126	3.5887	3.3793	3.2277	3.1068
		Mori-Tanaka	5.1528	3.7112	3.4440	3.2825	3.1459	3.0300

Table 8 Variation of fundamental frequency $\overline{\omega}$ with the power-law index p for FG beam

L/h	Theory		p					
			0	0.5	1	2	5	10
20	Ould Larbi *et al.* (2013)		5.4603	4.6511	4.2051	3.8361	3.6484	3.5389
	TBT (Simsek 2010)		5.4603	4.6511	4.2051	3.8361	3.6485	3.5390
	Present $(\boldsymbol{\varepsilon_z \neq 0})$	**Voigt**	**5.4603**	**4.6511**	**4.2051**	**3.8361**	**3.6484**	**3.5389**
		Reuss	**5.4603**	**3.8364**	**3.5956**	**3.4626**	**3.3350**	**3.2063**
		LRVE	**5.4603**	**4.1261**	**3.7815**	**3.5970**	**3.4765**	**3.3374**
		Tamura (q = 0)	**5.4603**	**3.8364**	**3.5956**	**3.4626**	**3.3350**	**3.2063**
		Tamura (q = 100)	**5.4603**	**4.1320**	**3.7998**	**3.6013**	**3.4696**	**3.3364**
		Mori-Tanaka	**5.4603**	**3.9258**	**3.6568**	**3.5070**	**3.3789**	**3.2468**

Table 8 shows the variations of the fundamental frequency $\overline{\omega}$ with power law index ($p = 0$, 0.5, 1, 2, 5, 10) and two span-to-depth ratios L/h. Effective Young's modulus is calculated using the aforementioned five micromechanical models. The obtained results are compared with those given by Simsek (2010) and the theory of Ould Larbi *et al.* (2013). From this table two observations can be made. First, the results obtained from the present hyperbolic beam theory (HBT) for the Voigt model are very close to those of Ould Larbi *et al.* (2013) and Simsek (2010). Secondly, the results from the present theory and calculated with the four other models, namely LRVE, Tamura, Mori-Tanaka and Reuss, are slightly different. This can be explained by the way of which the Young's modulus is calculated.

In Fig. 16, the variations of the non-dimensional fundamental natural frequency $\overline{\omega}$ versus the power law index p for a value of span-to-depth ratio $L/h = 5$ are given for different micromechanical models. It is seen from the figure that the increase of the power law index p produces a decrease in the values of the frequencies and this whatever the model used. The full ceramic beam ($p = 0$) presents the highest frequency for all models. However, the lowest
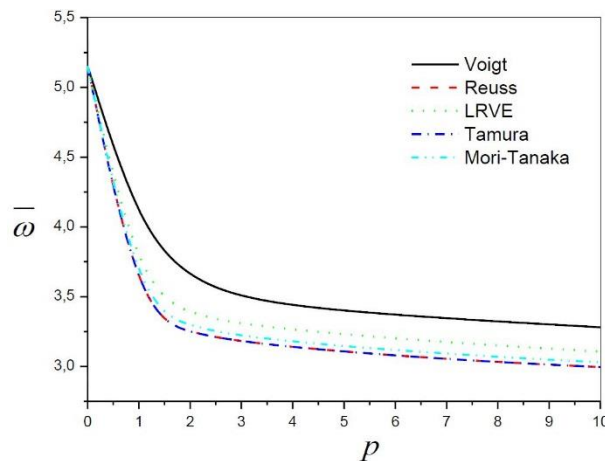

Fig. 16 Variation of the transverse shear stress $\overline{\tau}_{xz}$ through-the-thickness of a FG beam for different micromechanical models ($L/h = 2$, $p = 1$)

frequency values are obtained for full metal beams $(p \rightarrow \infty)$. In addition, the Voigt model has the highest frequencies values compared to other models, while that of Reuss has the lowest values. The Tamura and Reuss models have almost the same results.

Study 3: Free vibration analysis of embedded perfect and imperfect FG beams on elastic foundations

Figs. 17, 18, 19 and 20 present the variation of the non-dimensional fundamental frequency $\overline{\omega}$ of FG imperfect beams in function of the Winkler parameter and for three values of the porosity coefficient $\alpha = 0, \ 0.1 \ \text{and} \ 0.2$. It can be concluded that the influence of the Winkler parameter
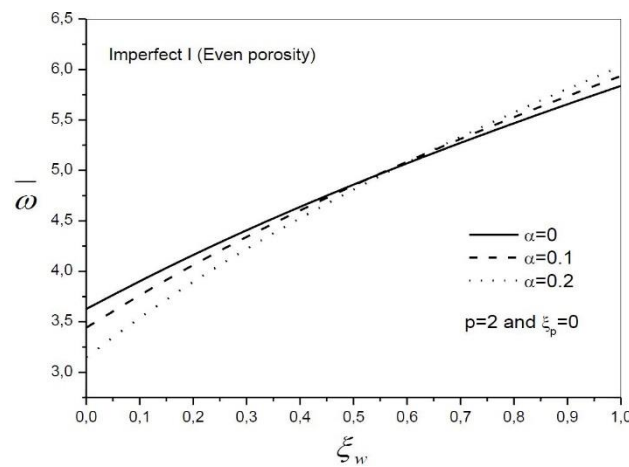
Fig. 17 Variation of the nondimensional fundamental frequency $\overline{\omega} = \frac{\omega L^2}{h} \sqrt{\frac{\rho_m}{E_m}}$ of FG beam with Winkler parameter ξ_w and porosity coefficient α
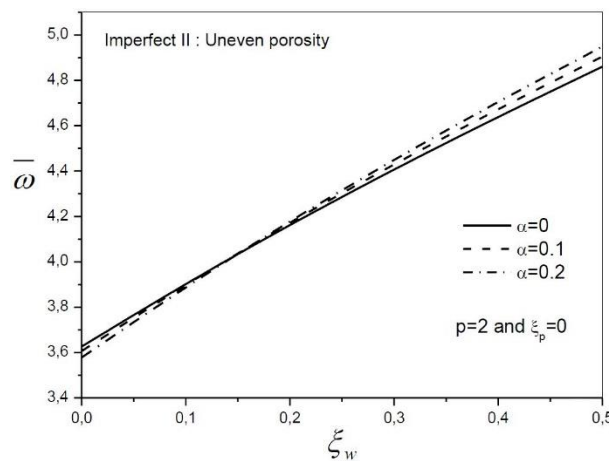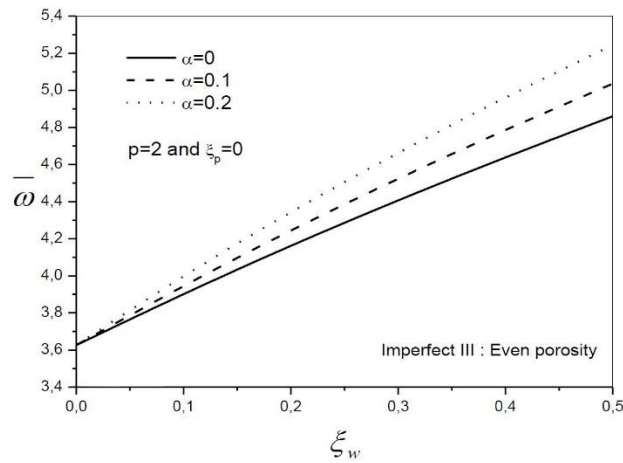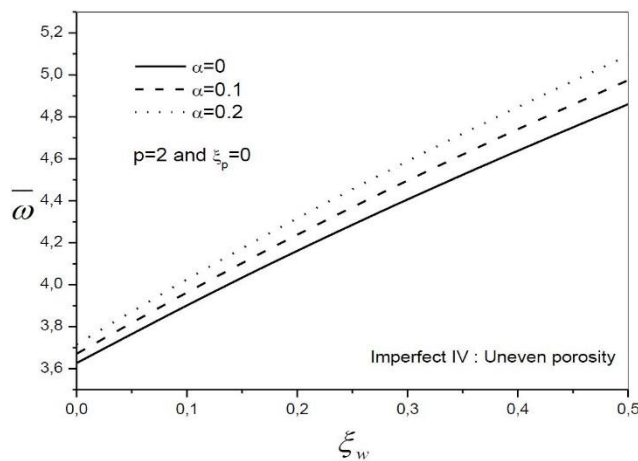

Fig. 18 Variation of the nondimensional fundamental frequency $\overline{\omega} = \frac{\omega L^2}{h} \sqrt{\frac{\rho_m}{E_m}}$ of FG beam with Winkler parameter ξ_w and porosity coefficient α

Fig. 19 Variation of the nondimensional fundamental frequency $\overline{\omega} = \frac{\omega L^2}{h}\sqrt{\frac{\rho_m}{E_m}}$ of FG beam with

Winkler parameter ξ_w and porosity coefficient α

Fig. 20 Variation of the nondimensional fundamental frequency $\overline{\omega} = \frac{\omega L^2}{h}\sqrt{\frac{\rho_m}{E_m}}$ of FG beam with

Winkler parameter ξ_w and porosity coefficient α

and the porosity on the frequency of imperfect beams with even porosities distribution (Imperfect I and III), and uneven porosities distributions (Imperfect II and IV) is very clear. It can be deduced from this curves that the highest the Winkler foundation parameter is, the highest the vibration frequency is, regardless the value of the porosity coefficient. Besides, an increase of the porosity coefficient leads to a higher vibration frequency.

Figs. 21, 22, 23 and 24 present the vibrational analysis of a short FG imperfect beam (even and uneven porosities distribution) and ($L/h = 5$) with consideration of the Pasternak effect. Three values of the porosity coefficient α are considered (0, 0.1 and 0.2). It can be deduced from this curve that the highest the Pasternak foundation parameter is, the highest the vibration frequency is,

regardless the value of the porosity coefficient. Besides, an increase of the porosity coefficient leads to a higher vibration frequency.

Fig. 25 present the variation of non-dimensional frequency $\overline{\omega}$ of embedded perfect and imperfect FG beams versus volume fraction indices p with $\alpha = 0.2$. It is pointed out that the natural frequencies decrease with the increase of the power law index p. This is due to the fact that an increase of the power law index p makes FG beams more flexible. It can be concluded that the influence of the porosity on the frequency of imperfect beams with even porosities distribution (Imperfect I and III), and uneven porosities distributions (Imperfect II and IV) is very clear. The even porosities distributions (Imperfect III), and the perfect beam have almost the same
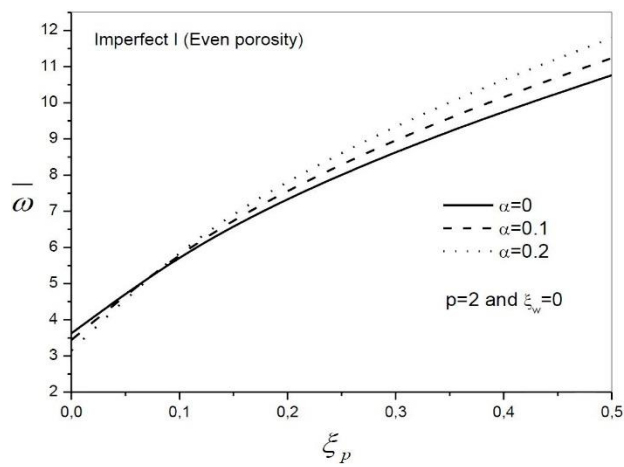

Fig. 21 Variation of the nondimensional fundamental frequency $\overline{\omega} = \frac{\omega L^2}{h} \sqrt{\frac{\rho_m}{E_m}}$ of FG beam with shear foundation parameter ξ_p and porosity coefficient α
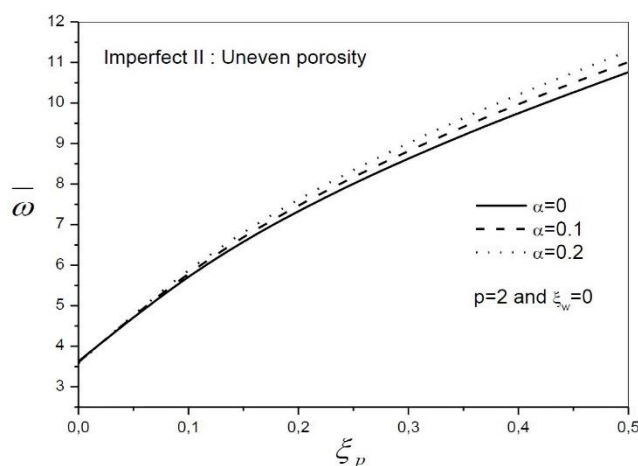

Fig. 22 Variation of the nondimensional fundamental frequency $\overline{\omega} = \frac{\omega L^2}{h} \sqrt{\frac{\rho_m}{E_m}}$ of FG beam with shear foundation parameter ξ_p and porosity. coefficient α
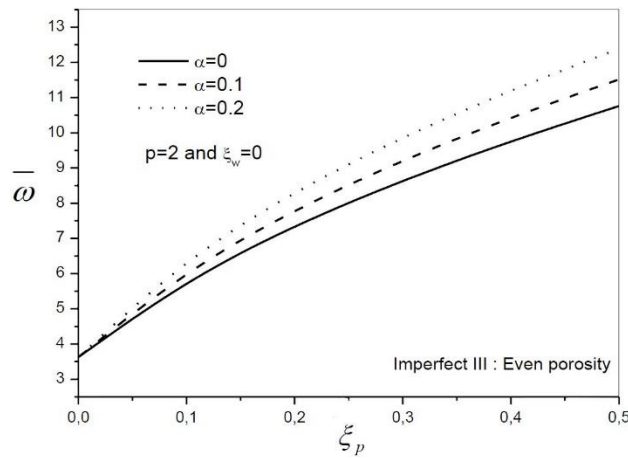
Fig. 23 Variation of the nondimensional fundamental frequency $\overline{\omega} = \dfrac{\omega L^2}{h}\sqrt{\dfrac{\rho_m}{E_m}}$ of FG beam with shear foundation parameter ξ_p and porosity coefficient α

Fig. 24 Variation of the nondimensional fundamental frequency $\overline{\omega} = \dfrac{\omega L^2}{h}\sqrt{\dfrac{\rho_m}{E_m}}$ of FG beam with shear foundation parameter ξ_p and porosity coefficient α

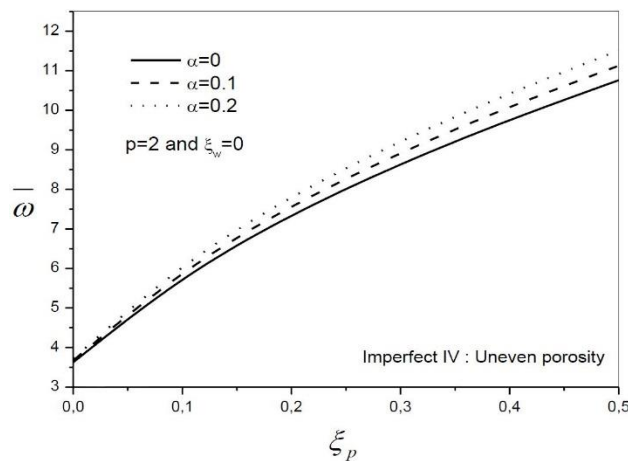frequencies. The difference between the results calculated with the four models of porosities, are slightly different. This can also be explained by the way who the Young's modulus is calculated.

5. Conclusions

The present work focuses on bending and free vibration analysis of perfect and imperfect FG beams under sinusoidal loads resting on two parameters elastic foundation by employing a simple higher order shear and normal deformation theory. The theory is developed by making further
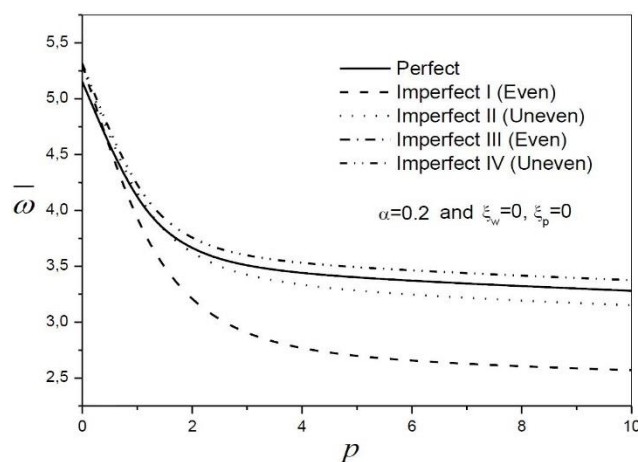
Fig. 25 Variation of non-dimensional frequency $\overline{\omega}$ of embedded perfect and imperfect FG beams versus volume fraction indices p ($\alpha = 0.2$ and $L/h = 5$)

simplifying assumptions to the existing HSDTs, with the use of an undetermined integral term. Different patterns of porosity distributions (including even and uneven distribution patterns, and the logarithmic-uneven pattern) are considered. In addition, the effect of different micromechanical models on the bending and free vibration response of these beams is studied. Various micromechanical models are used to evaluate the mechanical characteristics of the FG beams for which properties vary continuously across the thickness according to a simple power law. The equations of motion are obtained through the Hamilton's principle. These equations are solved by employing Navier's procedure. Subsequently the displacement, stress and fundamental frequencies are found by solving eigenvalue problem. For the new shear strain shape function usedin this paper, the obtained results are compared with those reported by various beam theories. The accuracy of the present theory is ascertained by comparing it with existing solutions and excellent agreement was observed in all cases. It is relevant to notice the strong effect of considering the nonzero transverse normal strain ε_z. Indeed, the inclusion of thickness stretching effect makes a beam stiffer, and hence, leads to a reduction of deflection and an increase of frequency. For the effect of foundation parameters, It is observed from results that the displacement and stresses of FG beam are reduced when it is resting on two parameter elastic foundation i.e., Winkler layer and shearing layer. Regarding the effect of effect of micromechanical models on bending and free vibration analysis of FG beams, we found that there is a good agreement between displacements and stresses using the different micromechanical models under sinusoidal load. The slight difference may be explained by the way that the Young's modulus is calculated.

In conclusion, it can be said that the present theory is not only accurate but also efficient in predicting displacements, stresses and natural frequency of both homogenous and FG beams. The extension of this study is also envisaged for general boundary conditions and different types of FG beams subjected to different loading (mechanical, thermal, buckling, etc.).

References

Abualnour, M., Chikh, A., Hebali, H., Kaci, A., Tounsi, A., Bousahla, A.A. and Tounsi, A. (2019), "Thermomechanical analysis of antisymmetric laminated reinforced composite plates using a new four variable trigonometric refined plate theory", *Comput. Concrete, Int. J.*, **24**(6), 489-498. https://doi.org/10.12989/cac.2019.24.6.489

Adda Bedia, W., Houari, M.S.A., Bessaim, A., Bousahla, A.A., Tounsi, A., Saeed, T. and Alhodaly, M.S. (2019), "A new hyperbolic two-unknown beam model for bending and buckling analysis of a nonlocal strain gradient nanobeams", *J. Nano Res.*, **57**, 175-191. https://doi.org/10.4028/www.scientific.net/JNanoR.57.175

Addou, F.Y., Meradjah, M., Bousahla, A.A., Benachour, A., Bourada, F., Tounsi, A. and Mahmoud, S.R. (2019), "Influences of porosity on dynamic response of FG plates resting on Winkler/Pasternak/Kerr foundation using quasi 3D HSDT", *Comput. Concrete, Int. J.*, **24**(4), 347-367. https://doi.org/10.12989/cac.2019.24.4.347

Ait Atmane, H., Tounsi, A. and Bernard, F. (2017), "Effect of thickness stretching and porosity on mechanical response of a functionally graded beams resting on elastic foundations", *Int. J. Mech. Mater. Des.*, **13**(1), 71-84. https://doi.org/10.1007/s10999-015-9318-x

Ait Yahia, S., Ait Atmane, H., Houari, M.S.A. and Tounsi, A. (2015), "Wave propagation in functionally graded plates with porosities using various higher-order shear deformation plate theories", *Struct. Eng. Mech., Int. J.*, **53**(6), 1143-1165. https://doi.org/10.12989/sem.2015.53.6.1143

Akbarzadeh, A.H., Abedini, A. and Chen, Z.T. (2015), "Effect of micromechanical models on structural responses of functionally graded plates", *Compos. Struct.*, **119**, 598-609. https://doi.org/10.1016/j.compstruct.2014.09.031

Akbaş, S.D. (2017), "Thermal effects on the vibration of functionally graded deep beams with porosity", *Int. J. Appl. Mech.nics*, **9**(5), 1750076. https://doi.org/10.1142/S1758825117500764

Alimirzaei, S., Mohammadimehr, M. and Tounsi, A. (2019), "Nonlinear analysis of viscoelastic micro-composite beam with geometrical imperfection using FEM: MSGT electro-magneto-elastic bending, buckling and vibration solutions", *Struct. Eng. Mech., Int. J.*, **71**(5), 485-502. https://doi.org/10.12989/sem.2019.71.5.485

Barretta, R., Feo, L., Luciano, R., Marotti de Sciarra, F. and Penna, R. (2016), "Functionally graded Timoshenko nanobeams: A novel nonlocal gradient formulation", *Compos. Part B*, **100**(1), 208-219. https://doi.org/10.1016/j.compositesb.2016.05.052

Barretta, R., Ali Faghidian, S., Luciano, R., Medaglia, C.M. and Penna, R. (2018), "Free vibrations of FG elastic Timoshenko nano-beams by strain gradient and stress-driven nonlocal models", *Compos. Part B*, **154**(1), 20-32. 10.1016/j.compositesb.2018.07.036

Batou, B., Nebab, M., Bennai, R., Ait Atmane, H., Tounsi, A., and Bouremana, M., (2019), "Wave dispersion properties in imperfect sigmoid plates using various HSDTs", *Steel Compos. Struct., Int. J.*, **33**(5), 699-716. https://doi.org/10.12989/scs.2019.33.5.699

Belbachir, N., Draiche, K., Bousahla, A.A., Bourada, M., Tounsi, A. and Mahmoud, S.R. (2019), "Bending analysis of anti-symmetric cross-ply laminated plates under nonlinear thermal and mechanical loadings", *Steel Compos. Struct., Int. J.*, **33**(1), 81-92. https://doi.org/10.12989/scs.2019.33.1.081

Berghouti, H., Adda Bedia, E.A., Benkhedda, A. and Tounsi, A. (2019), "Vibration analysis of nonlocal porous nanobeams made of functionally graded material", *Adv. Nano Res., Int. J.*, **7**(5), 351-364. https://doi.org/10.12989/anr.2019.7.5.351

Boukhlif, Z., Bouremana, M., Bourada, F., Bousahla, A.A., Bourada, M., Tounsi, A. and Al-Osta, M.A. (2019), "A simple quasi-3D HSDT for the dynamics analysis of FG thick plate on elastic foundation", *Steel Compos. Struct., Int. J.*, **31**(5), 503-516. https://doi.org/10.12989/scs.2019.31.5.503

Boulefrakh, L., Hebali, H., Chikh, A., Bousahla, A.A., Tounsi, A. and Mahmoud, S.R. (2019), "The effect of parameters of visco-Pasternak foundation on the bending and vibration properties of a thick FG plate", *Geomech. Eng., Int. J.*, **18**(2), 161-178. https://doi.org/10.12989/gae.2019.18.2.161

Bourada, F., Bousahla, A.A., Bourada, M., Azzaz, A., Zinata, A. and Tounsi, A. (2019), "Dynamic

investigation of porous functionally graded beam using a sinusoidal shear deformation theory", *Wind Struct.*, *Int. J.*, **28**(1), 19-30. https://doi.org/10.12989/was.2019.28.1.019

Boussoula, A., Boucham, B., Bourada, M., Bourada, F., Tounsi, A., Bousahla, A.A. and Tounsi, A. (2020), "A simple nth-order shear deformation theory for thermomechanical bending analysis of different configurations of FG sandwich plates", *Smart Struct. Syst.*, *Int. J.*, **25**(2), 197-218. https://doi.org/10.12989/sss.2020.25.2.197

Boutaleb, S., Benrahou, K.H., Bakora, A., Algarni, A., Bousahla, A.A., Tounsi, A., Tounsi, A. and Mahmoud, S.R. (2019), "Dynamic analysis of nanosize FG rectangular plates based on simple nonlocal quasi 3D HSDT", *Adv. Nano Res.*, *Int. J.*, **7**(3), 191-208. https://doi.org/10.12989/anr.2019.7.3.191

Chaabane, L.A., Bourada, F., Sekkal, M., Zerouati, S., Zaoui, F.Z., Tounsi, A., Derras, A., Bousahla, A.A. and Tounsi, A. (2019), "Analytical study of bending and free vibration responses of functionally graded beams resting on elastic foundation", *Struct. Eng. Mech.*, *Int. J.*, **71**(2), 185-196. https://doi.org/10.12989/sem.2019.71.2.185

Delale, F. and Erdogan, F. (1983), "The crack problem for a nonhomogeneous plane", *J. Appl. Mech.*, **50**(6), 609-614. https://doi.org/10.1115/1.3167098

Ding, J.H., Huang, D.J. and Chen, W.Q. (2007), "Elasticity solutions for plane anisotropic functionally graded beams", *Int. J. Solids Struct.*, **44**(1), 176-196. https://doi.org/10.1016/j.ijsolstr.2006.04.026

Draiche, K., Bousahla, A.A., Tounsi, A., Alwabli, A.S., Tounsi, A. and Mahmoud, S.R. (2019), "Static analysis of laminated reinforced composite plates using a simple first-order shear deformation theory", *Comput. Concrete*, *Int. J.*, **24**(4), 369-378. https://doi.org/10.12989/cac.2019.24.4.369

Draoui, A., Zidour, M., Tounsi, A. and Adim, B. (2019), "Static and dynamic behavior of nanotubes-reinforced sandwich plates using (FSDT)", *J. Nano Res.*, **57**, 117-135. https://doi.org/10.4028/www.scientific.net/JNanoR.57.117

Gasik, M. (1995), "Scand. Ch226", *Acta Polytech*, **72**.

Guerroudj, H.Z, Yeghnem, R., Kaci, A., Zaoui, F.Z., Benyoucef, S. and Tounsi, A. (2018), "Eigenfrequencies of advanced composite plates using an efficient hybrid quasi-3D shear deformation theory", *Smart Struct. Syst.*, *Int. J.*, **22**(1), 121-132. https://doi.org/10.12989/sss.2018.22.1.121

Hassaine Daouadji, T., Henni, A.H., Tounsi, A. and Bedia, E.A.A. (2013), "Elasticity solution of a cantilever functionally graded beam", *Appl. Compos. Mater.*, **20**(1), 1-15. https://doi.org/10.1007/s10443-011-9243-6

Hassaine Daouadji, T., Adim, B. and Benferhat, R. (2016), "Bending analysis of an imperfect FGM plates under hygro-thermo-mechanical loading with analytical validation", *Adv. Mater. Res.*, *Int. J.*, **5**(1), 35-53. https://doi.org/10.12989/amr.2016.5.1.035

Hellal, H., Bourada, M., Hebali, H., Bourda, F., Tounsi, A., Bousahla, A.A. and Mahmour, S.R. (2019), "Dynamic and stability analysis of functionally graded material sandwich plates in hygro-thermal environment using a simple higher shear deformation theory", *J. Sandw. Struct. Mater.* https://doi.org/10.1177/1099636219845841

Hussain, M., Naeem, M.N., Tounsi, A. and Taj, M. (2019), "Nonlocal effect on the vibration of armchair and zigzag SWCNTs with bending rigidity", *Adv. Nano Res.*, *Int. J.*, **7**(6), 431-442. https://doi.org/10.12989/anr.2019.7.6.431

Jaesang, Y. and Addis, K. (2014), "Modeling functionally graded materials containing multiple heterogeneities", *Acta Mech.*, **225**(7), 1931-1943. https://doi.org/10.1007/s00707-013-1033-9

Jha, D.K., Kant, T. and Singh, R.K. (2013), "Critical review of recent research on functionally graded plates", *Compos. Struct.*, **96**, 833-849. https://doi.org/10.1016/j.compstruct.2012.09.001

Ju, J. and Chen, T.M. (1994), "Micromechanics and effective moduli of elastic composites containing randomly dispersed ellipsoidal inhomogeneities", *Acta Mech.*, **103**(1-4), 103-121. https://doi.org/10.1007/BF01180221

Karama, M., Afaq, K.S. and Mistou, S. (2003), "Mechanical behavior of laminated composite beam by new multi-layered laminated Compos Struct model with transverse shear stress continuity", *Int. J. Solids Struct.*, **40**(6), 1525-1546. https://doi.org/10.1016/S0020-7683(02)00647-9

Karami, B., Janghorban, M. and Li, L. (2017), "On guided wave propagation in fully clamped porous

functionally graded nanoplates", *Acta Astronautica*, **143**, 380-390.
https://doi.org/10.1016/j.actaastro.2017.12.011

Karami, B., Janghorban, M., Shahsavari, D. and Tounsi, A. (2018a), "A size-dependent quasi-3D model for wave dispersion analysis of FG nanoplates", *Steel Compos. Struct.*, *Int. J.*, **28** (1), 99-110.
https://doi.org/10.12989/scs.2018.28.1.099

Karami, B., Janghorban, M. and Janghorban, M. (2018b), "Wave propagation analysis in functionally graded (FG) nanoplates under in-plane magnetic field based on nonlocal strain gradient theory and four variable refined plate theory", *Mech. Adv. Mater. Struct.*, **25**(12), 1047-1057.
https://doi.org/10.1080/15376494.2017.1323143

Karami, B., Janghorban, M. and Tounsi, A. (2019a), "Galerkin's approach for buckling analysis of functionally graded anisotropic nanoplates/different boundary conditions", *Eng. Comput.*, **35**, 1297-1316.
https://doi.org/10.1007/s00366-018-0664-9

Karami, B., Shahsavari, D., Janghorban, M. and Tounsi, A. (2019b), "Resonance behavior of functionally graded polymer composite nanoplates reinforced with grapheme nanoplatelets", *Int. J. Mech. Sci.*, **156**, 94-105. https://doi.org/10.1016/j.ijmecsci.2019.03.036

Karami, B., Janghorban, M. and Tounsi, A. (2019c), "On exact wave propagation analysis of triclinic material using three dimensional bi-Helmholtz gradient plate model", *Struct. Eng. Mech.*, *Int. J.*, **69**(5), 487-497. https://doi.org/10.12989/sem.2019.69.5.487

Karami, B., Janghorban, M. and Tounsi, A. (2019d), "On pre stressed functionally graded anisotropic nanoshell in magnetic field", *J. Brazil. Soc. Mech. Sci. Eng.*, **41**(11), 495.
https://doi.org/10.1007/s40430-019-1996-0

Karami, B., Shahsavari, D., Janghorban, J. and Li, L. (2019e), "Influence of homogenization schemes on vibration of functionally graded curved microbeams", *Compos. Struct.*, **216**(15), 67-79.
https://doi.org/10.1016/j.compstruct.2019.02.089

Karami, B., Janghorban, M. and Rabczuk, T. (2019f), "Static analysis of functionally graded anisotropic nanoplates using nonlocal strain gradient theory", *Compos. Struct.*, **227**, 111249.
https://doi.org/10.1016/j.compstruct.2019.111249

Karami, B., Janghorban, M. and Tounsi, A. (2019g), "Wave propagation of functionally graded anisotropic nanoplates resting on Winkler-Pasternak foundation", *Struct. Eng. Mech.*, *Int. J.*, **7**(1), 55-66.
https://doi.org/10.12989/sem.2019.70.1.055

Karami, B., Janghorban, M. and Rabczuk, T. (2020a), "Dynamics of two-dimensional functionally graded tapered Timoshenko nanobeam in thermal environment using nonlocal strain gradient theory", *Compos. Part B*: *Eng.*, **182**(1), 107622. https://doi.org/10.1016/j.compositesb.2019.107622

Karami, B., Janghorban, M. and Tounsi, A. (2020b), "Novel study on functionally graded anisotropic doubly curved nanoshells", *Eur. Phys. J. Plus*, **135**(1), 103. https://doi.org/10.1140/epjp/s13360-019-00079-y

Karami, B., Shahsavari, D., Janghorban, M. and Li, L. (2020c), "Free vibration analysis of FG nanoplate with poriferous imperfection in hygrothermal environment", *Struct. Eng. Mech.*, *Int. J.*, **73**(2), 191-207.
https://doi.org/10.12989/sem.2020.73.2.191

Kendall, K., Howard, A., Birchall, J., Prat, P., Proctor, A. and Jefferies, S.A. (1983), "The relation between porosity, microstructure and strength, and the approach to advanced cement-based materials", *Phil. Trans. Roy. Soc. Lond. A*, **310**(1511), 139-153. https://doi.org/10.1098/rsta.1983.0073

Khelifa, Z., Hadji, L., Hassaine Daouadji, T. and Bourada, M. (2018), "Buckling response with stretching effect of carbon nanotube-reinforced composite beams resting on elastic foundation", *Struct. Eng. Mech.*, *Int. J.*, **67**(2), 125-130. https://doi.org/10.12989/sem.2018.67.2.125

Khiloun, M., Bousahla, A.A., Kaci, A., Bessaim, A., Tounsi, A. and Mahmoud, S.R. (2019), "Analytical modeling of bending and vibration of thick advanced composite plates using a four-variable quasi 3D HSDT", *Eng. Comput.*, 1-15. https://doi.org/10.1007/s00366-019-00732-1

Kitipornchai, S., Yang, J. and Liew, K.M. (2006), "Random vibration of the functionally graded laminates in thermal environments", *Comput. Meth. Appl. Mech. Eng.*, **195**, 1075-1095.
https://doi.org/10.1016/j.cma.2005.01.016

Mahmoud, S.R. and Tounsi, A. (2019), "On the stability of isotropic and composite thick plates", *Steel*

Compos. Struct., *Int. J.*, **33**(4), 551-568. https://doi.org/10.12989/scs.2019.33.4.551

Mahmoudi, A., Benyoucef, S., Tounsi, A., Benacour, A., Adda Bedia, E.A. and Mahmoud, S.R. (2019), "A refined quasi-3D shear deformation theory for thermo-mechanical behavior of functionally graded sandwich plates on elastic foundations", *J. Sandw. Struct. Mater.*, **21**(6), 1906-1926. https://doi.org/10.1177/1099636217727577

Mantari, J.L., Oktem, A.S. and Soares, C.G. (2012), "A new higher order shear deformation theory for sandwich and composite laminated plates" *Compos. Part B Eng.*, **43**(3), 1489-1499. https://doi.org/10.1016/j.compositesb.2011.07.017

Mantari, J.L., Bonilla, E.M. and Guedes, S.C. (2014), "A new tangential-exponential higher order shear deformation theory for advanced composite plates", *Compos. Part B*, **60**, 319-328. https://doi.org/10.1016/j.compositesb.2013.12.001

Mantari, J.L., Ramos, I.A., Carrera, E. and Petrolo, M. (2016), "Static analysis of functionally graded plates using new nonpolynomial displacement fields via Carrera Unified Formulation", *Compos. Part B*, **89**, 127-142. https://doi.org/10.1016/j.compositesb.2015.11.025

Mechab, I., El Meiche, N. and Bernard, F. (2017), "Analytical study for the development of a new warping function for high order beam theory", *Compos. Part B*, **119**, 18-31. https://doi.org/10.1016/j.compositesb.2017.03.006

Medani, M., Benahmed, A., Zidour, M., Heireche, H., Tounsi, A., Bousahla, A.A., Tounsi, A. and Mahmoud, S.R. (2019), "Static and dynamic behavior of (FG-CNT) reinforced porous sandwich plate", *Steel Compos. Struct.*, *Int. J.*, **32**(5), 595-610. https://doi.org/10.12989/scs.2019.32.5.595

Meksi, R., Benyoucef, S., Mahmoudi, A., Tounsi, A., Adda Bedia, E.A. and Mahmoud, S.R. (2019), "An analytical solution for bending, buckling and vibration responses of FGM sandwich plates", *J. Sandw. Struct. Mater.*, **21**(2), 727-757. https://doi.org/10.1177/1099636217698443

Mishnaevsky, J.L. (2007), *Computational Mesomechanics of Composites*: *Numerical analysis of the effect of microstructures of composites on their strength and damage resistance*, John Wiley & Sons, UK. https://doi.org/10.1002/9780470513170

Neves, A.M.A., Ferreira, A.J.M., Carrera, E., Roque, C.M.C., Cinefra, M., Jorge, R.M.N. and Soares, C.M.M. (2012), "A quasi-3D hyperbolic shear deformation theory for the static and free vibration analysis of functionally graded plates", *Compos. Struct.*, **94**(5), 1814-1825. https://doi.org/10.1016/j.compstruct.2011.12.005

Ould Larbi, L., Kaci, A., Houari, M.S.A. and Tounsi, A. (2013), "An efficient shear deformation beam theory based on neutral surface position for bending and free vibration of functionally graded beams", *Mech. Bas. Des. Struct. Mach.*, **41**, 421-433. https://doi.org/10.1080/15397734.2013.763713

Reddy, J.N. (1984), "A simple higher order theory for laminated composite plates", *ASME J. Appl. Mech.*, **51**(4), 745-752. https://doi.org/10.1115/1.3167719

Sahla, M., Saidi, H., Draiche, K., Bousahla, A.A., Bourada, F. and Tounsi, A. (2019), "Free vibration analysis of angle-ply laminated composite and soft core sandwich plates", *Steel Compos. Struct.*, *Int. J.*, **33**(5), 663-679. https://doi.org/10.12989/scs.2019.33.5.663

Salah, F., Boucham, B., Bourada, F., Benzair, A., Bousahla, A.A. and Tounsi, A. (2019), "Investigation of thermal buckling properties of ceramic-metal FGM sandwich plates using 2D integral plate model", *Steel Compos. Struct.*, *Int. J.*, **33**(6), 805-822. https://doi.org/10.12989/scs.2019.33.6.805

Sallai, B.O., Tounsi, A., Mechab, I., Bachir, B.M., Meradjah, M. and Adda Bedia, E.A. (2009), "A theoretical analysis of flexional bending of Al/Al2O3 S-FGM thick beams", *Computat. Mater. Sci.*, **44**(4), 1344-1350. https://doi.org/10.1016/j.commatsci.2008.09.001

Shahsavari, D., Shahsavari, M., Li, L. and Karami, B. (2018), "A novel quasi-3D hyperbolic theory for free vibration of FG plates with porosities resting on Winkler/Pasternak/Kerr foundation", *Aerosp. Sci. Technol.*, **72**, 134-149. https://doi.org/10.1016/j.ast.2017.11.004

She, G.L., Yuan, F.G., Karami, B., Ren, Y.R. and Xiao, W.S. (2019), "On nonlinear bending behavior of FG porous curved nanotubes", *Int. J. Eng. Sci.*, **135**, 58-74. https://doi.org/10.1016/j.ijengsci.2018.11.005

Sayyad, A.S. and Ghugal, Y.M. (2017), "A unified shear deformation theory for the bending of isotropic, functionally graded, laminated and sandwich beams and plates", *Int. J. Appl. Mech.*, **9**(1), 1-36.

https://doi.org/10.1142/S1758825117500077

Sayyad, A.S. and Ghugal, Y.M. (2018), "An inverse hyperbolic theory for FG beams resting on Winkler-Pasternak elastic foundation", *Adv. Aircr. Spacecr. Sci.*, *Int. J.*, **5**(6), 671-689. https://doi.org/10.12989/aas.2018.5.6.671

Sayyad, A.S., Ghugal, Y.M. and Naik, N.S. (2015), "Bending analysis of laminated composite and sandwich beams according to refined trigonometric beam theory", *Curved Layer. Struct.*, **2**(1), 279-289. https://doi.org/10.1515/cls-2015-0015

Semmah, A., Heireche, H., Bousahla, A.A. and Tounsi, A. (2019), "Thermal buckling analysis of SWBNNT on Winkler foundation by non local FSDT", *Adv. Nano Res.*, *Int. J.*, **7**(2), 89-98. https://doi.org/10.12989/anr.2019.7.2.089

Shahsavari, D., Karami, B. and Li, L. (2018), "A high-order gradient model for wave propagation analysis of porous FG nanoplates", *Steel Compos. Struct.*, *Int. J.*, **29**(1), 53-66. https://doi.org/10.12989/scs.2018.29.1.053

Shen, H.S. and Wang, Z.X. (2012), "Assessment of Voigt and Mori-Tanaka models for vibration analysis of functionally graded plates", *Compos. Struct.*, **94**(7), 2197-2208. https://doi.org/10.1016/j.compstruct.2012.02.018

Simsek, M. (2010), "Fundamental frequency analysis of functionally graded beams by using different higher-order beam theories", *Nucl. Eng. Des.*, **240**(4), 697-705. https://doi.org/10.1016/j.nucengdes.2009.12.013

Soldatos, K.P. (1992), "A transverse shear deformation theory for homogeneous monoclinic plates", *Acta Mech.*, **94**(3-4), 195-220. https://doi.org/10.1007/BF01176650

Thai, H.T. and Choi, D.H. (2012), "A refined shear deformation theory for free vibration of functionally graded plates on elastic foundation", *Compos. Part B*, **43**, 2335-2347. https://doi.org/10.1016/j.compositesb.2011.11.062

Timoshenko, S.P. (1921), "On the correction for shear of the differential equation for transverse vibrations of prismatic bars", *Philos. Mag.*, **41**(245), 742-746. https://doi.org/10.1080/14786442108636264

Tlidji, Y., Zidour, M., Draiche, K., Safa, A., Bourada, M., Tounsi, A., Bousahla, A.A. and Mahmoud, S.R. (2019), "Vibration analysis of different material distributions of functionally graded microbeam", *Struct. Eng. Mech.*, *Int. J.*, **69**(6), 637-649. https://doi.org/10.12989/sem.2019.69.6.637

Touratier, M. (1991), "An efficient standard plate theory", *Int. J. Eng. Sci.*, **29**(8), 901-916. https://doi.org/10.1016/0020-7225(91)90165-Y

Wattanasakulpong, N. and Ungbhakorn, V. (2014), "Linear and nonlinear vibration analysis of elastically restrained ends FGM beams with porosities'', *Aerosp. Sci. Technol.*, **32**(1), 111-120. https://doi.org/10.1016/j.ast.2013.12.002

Wattanasakulpong, N., Prusty, B.G., Kelly, D.W. and Hoffman, M. (2012), "Free vibration analysis of layered functionally graded beams with experimental validation", *Mater. Des*, **36**, 182-190. https://doi.org/10.1016/j.matdes.2011.10.049

Ying, J., Lu, C.F. and Chen, W.Q. (2008), "Two-dimensional elasticity solutions for functionally graded beams resting on elastic foundations", *Compos. Struct.*, **84**(3), 209-219. https://doi.org/10.1016/j.compstruct.2007.07.004

Zaoui, F.Z., Ouinas, D. and Tounsi, A. (2019), "New 2D and quasi-3D shear deformation theories for free vibration of functionally graded plates on elastic foundations", *Compos. Part B*, **159**, 231-247. https://doi.org/10.1016/j.compositesb.2018.09.051

Zarga, D., Tounsi, A., Bousahla, A.A., Bourada, F. and Mahmoud, S.R. (2019), "Thermomechanical bending study for functionally graded sandwich plates using a simple quasi-3D shear deformation theory", *Steel Compos. Struct.*, *Int. J.*, **32**(3), 389-410. https://doi.org/10.12989/scs.2019.32.3.389

Zhu, J., Lai, Z., Yin, Z., Jeon, J. and Lee, S. (2001), "Fabrication of ZrO_2–NiCr functionally graded material by powder metallurgy", *Mater. Chem. Phys.*, **68**(1-3), 130-135. https://doi.org/10.1016/S0254-0584(00)00355-2

Zimmerman, R.W. (1994), "Behavior of the Poisson ratio of a two-phase composite material in the high-concentration limit", *Appl. Mech. Rev.*, **47**(1), 38-44. https://doi.org/10.1115/1.3122819

Zouatnia, N. and Hadji, L. (2019), "Effect of the micromechanical models on the bending of FGM beam using a new hyperbolic shear deformation theory", *Earthq. Struct.*, *Int. J.*, **16**(2), 177-183. https://doi.org/10.12989/eas.2019.16.2.177

Zouatnia, N., Hadji, L. and Kassoul, A. (2017), "An analytical solution for bending and vibration responses of functionally graded beams with porosities", *Wind Struct.*, *Int. J.*, **25**(4), 329-3420. https://doi.org/10.12989/was.2017.25.4.329

CC